

AFRPL-TR-72-56

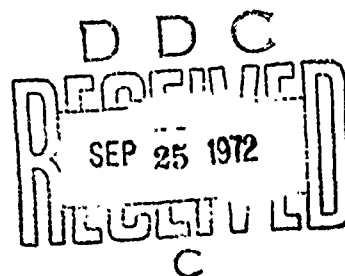
# A STUDY OF THE PROPULSION PERFORMANCE FROM PLASTICIZED EXPLOSIVES

R.F.BESTGEN, CAPT, USAF

I.R.NUNN, CAPT, USAF

TECHNICAL REPORT AFRPL-TR-72-56

AUGUST 1972



This document has been approved for public  
release and sale; its distribution is unlimited.

Reproduced by  
NATIONAL TECHNICAL  
INFORMATION SERVICE  
U S Department of Commerce  
Springfield VA 22151

AIR FORCE ROCKET PROPULSION LABORATORY  
DIRECTOR OF LABORATORIES  
AIR FORCE SYSTEMS COMMAND  
UNITED STATES AIR FORCE  
EDWARDS, CALIFORNIA

AD 748843

# NOTICES

When U.S. Government drawings, specifications, or other data are used for any purpose other than a definitely related Government procurement operation, the Government thereby incurs no responsibility, nor any obligation whatsoever, and the fact that the Government may have formulated, furnished or in any way supplied the said drawings, specifications, or other data, is not to be regarded by implication or otherwise, or in any manner as licensing the holder or any other person or corporation, or conveying any rights or permission to manufacture, use, or sell any patented invention that may in any way be related thereto.

ACCESSION for	
NTIS	White Section <input checked="" type="checkbox"/>
DDC	Buff Section <input type="checkbox"/>
UNANNOUNCED	<input type="checkbox"/>
JUSTIFICATION .....	
BY .....	
DISTRIBUTION/AVAILABILITY CODES	
Dist.	A-ALL, REG/CR SPECIAL
A	

AFRPL-TR-72-56

A STUDY OF THE PROPULSION  
PERFORMANCE FROM PLASTICIZED EXPLOSIVES

R. F. Bestgen, Capt, USAF  
J. R. Nunn, Capt, USAF

August 1972

This document has been approved for public  
release and sale; its distribution is unlimited.

AIR FORCE ROCKET PROPULSION LABORATORY  
DIRECTOR OF LABORATORIES  
AIR FORCE SYSTEMS COMMAND  
UNITED STATES AIR FORCE  
EDWARDS, CALIFORNIA

## FOREWORD

This is a report on work conducted at the Air Force Rocket Propulsion Laboratory during the period of October 1971 to May 1972. Capt R.F. Bestgen was the principal investigator and Capt J.R. Nunn performed the computer analysis.

This technical report has been reviewed and is approved.

PAUL J. DAILY, Lt Colonel, USAF  
Chief, Technology Division  
Air Force Rocket Propulsion Laboratory

## ABSTRACT

A theoretical study was made to determine the performance of a detonation propulsion system using plasticized explosives. Steady-state and shock-hydrodynamic calculations were completed for: (1) free-expansion detonations, where the explosive gases are free to expand from the vehicle mass after impacting the vehicle, (2) confined detonations, where recoil mass is used to constrain the expansion, and (3) totally confined detonations, where the momentum transfer to the vehicle mass and the conversion of detonation energy into vehicle kinetic energy are maximized. The effects upon propulsion performance of separating explosive charges from the vehicle mass, giving the explosive charge an initial velocity, and stacking explosive charges between solid materials, were also studied. Results show that a free-expansion detonation delivers a specific impulse comparable to that of a conventional chemical rocket using solid propellant. Separating the explosive charge from the vehicle can result in a moderate increase in the performance of a detonation propulsion system. Giving the explosive an initial velocity also increases performance, although this may be of marginal practical utility. Partially confining a detonation with material increases the momentum transfer to the vehicle and the vehicle's kinetic energy, but the confinement is not comparable to adding an equivalent amount of explosive mass. Stacking explosives between materials leads to a similar result. A totally confined detonation delivers the maximum performance from a detonation propulsion system, but vehicle damage is likely when using a totally confined detonation. The results indicate that the detonation propulsion concept is feasible for special purpose applications where the specific impulse required is about 250 to 300 seconds.

## TABLE OF CONTENTS

<u>Section</u>	<u>Page</u>
I INTRODUCTION . . . . .	1
II ANALYTICAL APPROACH. . . . .	3
Steady-State Approach. . . . .	3
Shock-Hydrodynamics Approach . . . . .	6
III RESULTS AND DISCUSSION. . . . .	9
Free-Expansion Detonations. . . . .	9
Explosive Mass Standoff . . . . .	13
Velocity-Boosted Charges . . . . .	14
Confined Detonations. . . . .	15
Totally Confined Detonations . . . . .	17
Test Results . . . . .	19
IV CONCLUSIONS AND RECOMMENDATIONS . . . . .	20
REFERENCES . . . . .	22
AUTHORS' BIOGRAPHIES . . . . .	23
APPENDIX . . . . .	25

Preceding page blank

## LIST OF ILLUSTRATIONS

<u>Figure</u>		<u>Page</u>
1	Detonation Propulsion System Schematic . . . . .	25
2	Shock-Hydrodynamics Computer Printout . . . . .	26
3	Free-Expansion Velocity and Density Distributions . .	27
4	Free-Expansion Detonation Specific Impulse . . . . .	28
5	Vehicle Mass Velocity History . . . . .	29
6	Pressure History (Free-Expansion Detonation) . . . .	30
7	Energy History (Compound B and Steel, Free-Expansion Detonation). . . . .	31
8	Explosive Mass Standoff Performance . . . . .	32
9	Velocity-Boosted Performance . . . . .	32
10	Confined Detonation Specific Impulse Performance . .	33
11	Stacked Explosives Performance Comparison. . . . .	34
12	Energy History (Compound B and Steel, Confined Detonation) . . . . .	35
13	Effect of Recoil Mass on Vehicle Mass Energy . . . .	36
14	Effect of Recoil Mass on Vehicle Mass Velocity. . . .	36
15	Pressure History Comparisons . . . . .	37
16	Energy History (Compound B and Steel, Totally Confined Detonation) . . . . .	38
17	Velocity Distribution Comparison . . . . .	39
18	Pressure History Comparison (Compound B and Steel). .	40
19	Vehicle Mass Velocity Comparison . . . . .	41
20	Specific Impulse Comparison . . . . .	42

## NOMENCLATURE

E	internal energy, calories
$E_0$	detonation energy/unit mass, cal/gm
F	burn fraction
g	gravitational constant, cm/sec <sup>2</sup>
I	impulse, dyne sec
I <sub>sp</sub>	specific impulse, seconds
J	element designator
$L^1$	standoff distance, centimeters
L	explosive charge length, centimeters
$l$	extent of explosive gases, centimeters
$M^1$	confining mass, grams
M	vehicle mass, grams
m	explosive mass of mass expended, grams
P	pressure, kilobars
Q	artificial viscosity term, kilobars
T, t	time, microseconds
U	vehicle mass velocity, cm/ $\mu$ s
u	gas velocity, cm/ $\mu$ s
ub	boost velocity, cm/ $\mu$ s
V	relative volume ( $\rho_0/\rho$ )
X	Eulerian coordinate, centimeters
x	Lagrangean coordinate, centimeters
$\gamma$	adiabatic exponent
$\rho$	density, gm/cm <sup>3</sup>

### Subscripts

cm	center-of-mass
e	elastic
o	reference
p	plastic
rms	root-mean-square

## SECTION I INTRODUCTION

The possibility of propelling a vehicle mass by the chemical energy release from a detonation is conceptually attractive. In principle, the explosive energy release is used to impart an impulse to the vehicle mass, increasing the vehicle's momentum. This technique differs from the use of conventional propellants in that a pressure vessel and nozzle are not necessary to convert energy into vehicle momentum. Extremely high pressures existing in the vicinity of the reaction zone of an explosive lead to rapid propulsive response, accompanied by short, controlled action times as the explosive energy is used to deliver an impulse.

Many potential propulsion applications require rapid response and short, controlled time performance. A detonation propulsion system using plasticized explosives might lead to the possibility of a simpler, lighter-weight, less-expensive, and better-performing vehicle than one which incorporates a more conventional propulsion system. Other applications of a detonation propulsion system include side-thrusting a missile or projectile and, on certain planetary probes, using the system for maneuvering where the atmospheric pressure is so high that conventional propulsion systems are ineffective.

The basic feasibility associated with the use of explosive charges in a propulsion device has not been determined. The physics of the interaction between the explosive gases and the vehicle mass has not been treated to the extent where either propulsion performance or vehicle mass response can be ascertained in detail. Both of these areas require investigation before serious mission or application studies are undertaken.

Considering the vehicle response first, it is generally the case that a detonation process results in stagnation pressures in the hundreds-of-kilobars range. At the gas-vehicle interface and throughout the vehicle

mass, stresses are propagated as a result of these pressures. Severe damage to the vehicle can result. The vehicle is also loaded to extreme gravitational force levels during the action time. The feasibility of employing materials between the explosive charges and the main vehicle structure to attenuate pressure levels (absorb energy) or to shape pressure waves has not been studied.

Little has been accomplished in determining the limiting features of propulsion performance of a detonation propulsion system. The delivered specific impulse, the vehicle mass terminal velocity, and the efficiency of detonation energy conversion need to be determined for a variety of conditions. Parametric studies are needed to determine methods for effecting propulsion performance. Preliminary studies have been completed to assess the specific impulse performance from a detonation propulsion system where the explosive gases are free to expand from the vehicle mass (Ref. 1 and 2). The results of these studies are discordant, defying correlation; however, one study is presently being repeated with its scope appreciably extended (Ref. 3).

The purpose of this investigation is to study the physics of interaction between plasticized explosives and a vehicle mass and to predict the limits of propulsion performance of a detonation propulsion system. The investigation is limited to theoretical considerations with the ultimate goal of providing information to determine the potential of a detonation propulsion system.

## SECTION II ANALYTICAL APPROACH

The propulsion performance resulting from an explosive charge interacting with a vehicle mass can be analyzed using conventional rocket terms. The velocity gained by the vehicle mass from the explosive interaction,  $U$ , the time over which the impulse is delivered, the efficiency of converting chemical detonation energy into gas or vehicle kinetic energy, and the specific impulse per explosive pulse,  $I_{sp}$ , are all important characteristic parameters. Other factors, however, such as the residual internal energy within the vehicle mass as a result of transmitted shocks, become of consequence in a detonation propulsion system.

### STEADY-STATE APPROACH

It is of interest to obtain a simple understanding of the interaction between an explosive charge and a vehicle mass. Consider the schematic shown in Figure 1.\* An explosive charge of mass,  $m$ , is initiated against a vehicle of mass  $M$ . As time passes, the explosive gases interact with the solid interface and expand from the interface. Assuming a one-dimensional interaction, as  $t \rightarrow \infty$ , conservation of mass, momentum, and energy per unit area follow immediately as:

$$m = \int_0^{\ell} \rho(x) dx \quad (1)$$

$$MU = \int_0^{\ell} \rho(x) u(x) dx \quad (2)$$

$$mE_0 = 1/2 MU^2 + 1/2 \int_0^{\ell} \rho(x) u^2(x) dx \quad (3)$$

where  $E_0$  is the chemical detonation energy release per unit mass,  $\ell$  is the spatial extent of the explosive gases, and  $\rho(x)$  and  $u(x)$  are gas

---

\*Figures are presented in the Appendix, page 25.

density and velocity, respectively, as functions of position,  $x$ . Equations 1 through 3 apply to the case of a free-expansion detonation. If, for instance, material is used to confine the detonation, this must be taken into account in the momentum and energy balance. Under this more general condition, Equations 2 and 3 become

$$MU = M' U' + \int_0^{\ell} \rho(x) u(x) dx \quad (4)$$

$$mE_0 = 1/2 MU^2 + 1/2 M' U'^2 + 1/2 \int_0^{\ell} \rho(x) u^2(x) dx \quad (5)$$

where the primed superscripts denote the confining conditions. In writing Equations 3 and 5, energy converted to vehicle internal energy has been ignored. It is also noted that Equations 2 through 5 assume that the vehicle and confining masses are rigid.

Equations 1 through 3 may be solved simultaneously for a given explosive gas density and velocity distribution to yield an expression for vehicle terminal velocity as a function of detonation energy, explosive charge mass, and the vehicle mass. Or,

$$U = U(E_0, m, M) \quad (6-a)$$

For the more general case involving a confining mass, Equation 6-a is replaced with

$$U = U(E_0, m, M, M') \quad (6-b)$$

assuming that a condition can be written to relate the confining mass velocity to the vehicle velocity (Section III).

The specific impulse delivered as a result of a detonation interaction follows from conservation of impulse involving the explosive mass and the vehicle mass system. By definition,

$$I_{sp} = \frac{I}{gm} \quad (7)$$

where  $I$  is the impulse imparted and  $m$  the mass expended to impart the impulse. The gravitational constant,  $g$ , is included in Equation 7 to maintain conventional units for specific impulse. To avoid confusion, the mass  $m$  here may be the explosive charge mass yielding an equivalent specific impulse based upon the mass of explosive expended. The mass  $m$  may also include confining or other mass yielding an effective specific impulse based upon the total mass expended to impart an impulse. Clearly, these values may be different. The impulse imparted to the vehicle mass is the momentum change of the vehicle as a result of the detonation interaction. Or,

$$I = MU \quad (8-a)$$

Similarly for the explosive charge, the impulse magnitude is

$$I = mu \quad (8-b)$$

where  $m$  is the charge mass and  $u$  the final explosive gas velocity. From Equations 7 and 8

$$I_{sp} = \frac{U}{gm/M} = \frac{u}{g} \quad (9)$$

The conventional result given by Equation 9, relating specific impulse to gas velocity, is noted. Here, it is more convenient to relate specific impulse to vehicle terminal velocity. Combining Equations 6 and 9, it is seen that the specific impulse performance of a detonation propulsion

system is related to the detonation energy available, a finding consistent with conventional chemical rocket results.

An alternate steady-state approach allowing insight into the physics of interaction between an explosive charge and a vehicle mass involves treating the detonation as a compression wave reflecting from the vehicle mass. In this case, the conservation equations are employed across the compression wave. In addition, static gas properties along the wave are related with the space and time characteristics of the dynamic flow field. Combining these relationships with the reflected pressure, which gives rise to an acceleration of the vehicle mass, leads to a nonlinear differential expression. This expression has a solution for a gas with an adiabatic exponent  $\gamma = 3$ . As  $t \rightarrow \infty$ , the acceleration is zero and the vehicle mass has a terminal velocity with the functional form given by Equation 6 (Ref. 4).

#### SHOCK-HYDRODYNAMICS APPROACH

The steady-state treatment of the interaction between an explosive charge and a vehicle mass is approximate. The dynamics involving shocks and their interactions, and the resultant detailed behavior of the media concerned are obscured by analyzing only the asymptotic time behavior. The time history of material properties and their transient characteristics are of considerable importance. An accurate analytical approach must allow for this feature. Shock-hydrodynamics computer codes have been developed for this purpose.

The program used to determine dynamic behavior was a one-dimensional, time-dependent computer code using Lagrangean coordinate zoning of the explosive gas and vehicle mass system in which strong shocks are treated by the introduction of the Von Neumann and Richtmyer nonlinear viscosity (Ref. 5). The logic is based upon the conservation equations rewritten from partial differential expressions into equivalent finite difference equations subject to appropriate boundary

conditions. Numerical integrations are performed using space zoning and time steps chosen to satisfy the required stability conditions.

Figure 2 illustrates a typical computer printout at time  $T$ , in microseconds, from the initiation of an explosive charge with detonation energy  $E_0$ . The zoning increment for a given medium is designated by  $\bar{\Delta}$ , and  $X$  represents the position at time  $T$  of the medium element that was at position  $x$  initially. The element's velocity,  $u$ , the element's relative volume,  $V$  (given as the ratio of the initial density at position  $x$  to the density at position  $X$  at time  $T$ ), the element's static pressure,  $P$ , and the element's internal energy,  $E$ , all follow from the conservation equations and the equation of state describing the medium. The artificial viscosity,  $Q$ , indicates shock layers, and the burn fraction,  $F$ , represents the amount of material in an element that has detonated by virtue of the static pressure reaching the Chapman-Jouguet pressure. The kinetic energy and internal energy in a medium of given mass are also calculated for time  $T$ .

From the numerical solutions, the vehicle mass velocity at time  $T$  is given as the center-of-mass velocity determined by summing the element mass fraction and velocity products over all elements. The specific impulse at time  $T$  follows from Equation 9. The impulse imparted to the vehicle mass is given by the static pressure history in the gas element adjacent to the vehicle mass. The action time follows immediately with consideration given to the time over which the gas exerts a pressure influence on the vehicle mass. The spatial distribution and time dependency of the total energy throughout a given medium are also known from the numerical information. Thus, a complete description of the time dependent dynamic behavior of the interaction between an explosive charge or charges and a vehicle mass including confining materials or other masses is provided by the shock-hydrodynamics computer program. However, a shortcoming is noted for the program in that spallation, defined as material ejected from a medium as a result of stresses beyond the dynamic yield strength, is

been neglected. The effect of spallation is to decrease the effective specific impulse of a detonation propulsion system. The decrease in inefficiency is assumed to be small.

### SECTION III RESULTS AND DISCUSSION

The analyses performed herein considered two explosive materials and two solid mass materials. Detasheet (EL-506-C) and Compound B, Grade A were the explosive materials used with initial densities of  $1.47 \text{ gm/cm}^3$  and  $1.715 \text{ gm/cm}^3$ , adiabatic exponents of 2.70 and 2.77, detonation energies of  $0.0373 \text{ Mb-cm}^3/\text{gm}$  and  $0.0478 \text{ Mb-cm}^3/\text{gm}$ , and Chapman-Jouguet pressures of 186 kilobars and 292 kilobars, respectively. The solid mass materials used were steel and aluminum with initial densities of  $7.84 \text{ gm/cm}^3$  and  $2.7 \text{ gm/cm}^3$ , respectively. For steady-state calculations, the term  $\sqrt{2E_0}$  was assumed to be a constant with a magnitude of 8200 ft/sec ( $0.25 \text{ cm/microsecond}$ ), a value within the experimental scatter of data for Compound B (Ref. 2). For dynamic-state calculations, polynomial equations-of-state (in terms of the relative volume) were used for solid masses, and gamma law equations-of-state were used for the explosive gases (Ref. 6). Computer calculations were performed using an IBM 7040 and a CDC 6600.

#### FREE-EXPANSION DETONATIONS

The steady-state propulsion performance resulting from an explosive charge initiated against a vehicle mass with the explosive gases allowed to expand freely from the vehicle mass follows from Equations 1 to 3. The most common analysis assumes a constant explosive gas density with a linear gas velocity distribution given by:

$$u(x) = (u_\ell + U) \frac{x}{\ell} - U \quad (10)$$

where  $u_\ell$  is the gas velocity at distance  $\ell$ . Then Equations 1 to 3 yield:

$$U = \sqrt{2E_0} \sqrt{\frac{3(m/M)^2}{4 + 5m/M + (m/M)^2}} \quad (11)$$

and, using Equation 9,

$$I_{sp} = \frac{\sqrt{2E_0}}{g} \sqrt{\frac{3}{4 + 5 m/M + (m/M)^2}} \quad (12)$$

It is noted that Equation 10 assumes a no-slip velocity condition at the gas-vehicle mass interface. The general validity of assuming a constant gas density and a linear gas velocity distribution for times long after the initiation of the explosive charge can be verified from Figure 3 which illustrates typical computer results for Detasheet or Compound B freely expanding from a steel vehicle mass. The dubious validity of the no-slip velocity condition at the gas-vehicle mass interface can be seen from Figure 3. Nonetheless, Equations 11 and 12 describe the explicit dependence of propulsion performance on detonation energy, the explosive charge mass and the vehicle mass. The specific impulse per pulse asymptotes to a constant value when  $m/M \rightarrow 0$  and decreases as  $m/M$  increases. However, the vehicle terminal velocity increases monotonically with increasing  $m/M$  values.

The apparent limits of steady-state propulsion performance of a free-expansion detonation are obtained by using gas properties that simulate an elastic or a plastic interaction between the explosive gases and the vehicle mass. The simple gas density distributions given by

$$\rho(x) = \rho_0 \frac{x}{\ell} \quad (13-a)$$

and

$$\rho(x) = \rho_0 \left( 1 - \frac{x}{\ell} \right) \quad (13-b)$$

where  $\rho_0$  is a reference density are taken to represent the elastic and plastic interactions, respectively. These equations combined with Equations 1 and 3 and Equation 10 yield

$$U_e = \sqrt{2E_0} \sqrt{\frac{8 (m/M)^2}{9 + 10 m/M + (m/M)^2}} \quad (14-a)$$

and

$$U_p = \sqrt{2E_0} \sqrt{\frac{2 (m/M)^2}{3 + 4 m/M + (m/M)^2}} \quad (14-b)$$

where the subscripts e and p refer to elastic and plastic, respectively. The specific impulse per explosive pulse for these two cases follows immediately from Equation 9. From Equations 9 and 14,

$$\frac{I_{sp}^{(e)}}{I_{sp}^{(p)}} = \frac{U_e}{U_p} = 2 \sqrt{\frac{3 + 4 m/M + (m/M)^2}{9 + 10 m/M + (m/M)^2}} \quad (15)$$

and, as  $m/M \rightarrow 0$ ,  $\frac{I_{sp}^{(e)}}{I_{sp}^{(p)}} = \frac{U_e}{U_p} = 1.15$ , and as  $m/M \rightarrow \infty$ ,  $\frac{I_{sp}^{(e)}}{I_{sp}^{(p)}} = \frac{U_e}{U_p} = 2$ , the expected result.

The actual optimum in steady-state propulsion performance of a free-expansion detonation is given when the explosive gas velocity is constant. This holds for all the gas density distributions considered thus far, and presumably, for an arbitrary gas density distribution. That this is so follows by seeking that  $\rho(x)$  and  $U(x)$  which render the functional

$$\int_0^\ell \rho(x) u^2(x) dx \text{ a maximum subject to the side conditions that } \int_0^\ell \rho(x) dx = C_1$$

and  $\int_0^\ell \rho(x) v(x) dx = C_2$  where  $C_1$  and  $C_2$  are constants.

Then,

$$U = \sqrt{2E_o} \sqrt{\frac{(m/M)^2}{1 + m/M}} \quad (16-a)$$

and

$$I_{sp} = \frac{\sqrt{2E_o}}{g} \sqrt{\frac{1}{1 + m/M}} \quad (16-b)$$

Again, the specific impulse per explosive pulse asymptotes to a constant value when  $m/M \rightarrow 0$  and decreases as  $m/M$  increases. It is noted that the asymptotic value of specific impulse for the optimum steady-state performance case corresponds to the performance attainable from a conventional chemical rocket operating without loss. Again, for the optimum performance case the vehicle terminal velocity increases with increasing  $m/M$  values.

Figure 4 displays the specific impulse per pulse as a function of explosive mass to vehicle mass ratio predicted from Equations 12 and 16. This figure is for Compound B explosive and steel vehicle mass. The band reflecting Equation 14 is shown in Figure 4 at a mass ratio of  $10^{-2}$ . In addition, Figure 4 illustrates the steady-state performance predicted by considering the detonation as a compression wave reflecting from the vehicle mass (for a  $\gamma = 3$  gas). The computer results of References 1 and 2 are also shown in Figure 4. The computations of Reference 1 were based on the root-mean-square velocity of the vehicle mass determined from kinetic energy considerations. It is noted that  $U_{rms} > U_{cm}$ ; therefore,  $I_{sp})_{rms} > I_{sp})_{cm}$  by virtue of the relative motion of each of the material elements about the center-of-mass. The effect on specific impulse performance of using a 15-degree infinitely long nozzle is also shown in Figure 4. This result was taken from Reference 2. Lastly, Figure 4 displays the results of our shock-hydrodynamics calculations. The data points shown correspond to a time 100 microseconds after detonation

initiation. The scatter band about these data points denotes the time variation of the center-of-mass velocity of the vehicle mass. (See Figure 5, which also shows the history of the root-mean-square velocity.) From Figure 4, it is seen that a free-expansion detonation propulsion system delivers a specific impulse comparable to that of a conventional chemical rocket using solid propellant. Shifting equilibrium calculations using Compound B expanding from 1000 psi to 14.7 psi delivers approximately 255 seconds specific impulse for an optimally designed rocket (Ref. 7). Specific impulse performance of nominally 240 to 250 seconds appears possible from a free-expansion detonation propulsion system using conventional plasticized explosives like Compound B at low mass ratios. This prediction assumes that two-dimensional effects upon performance are of second-order magnitude and that spallation from the vehicle mass and vehicle damage are negligible.

Figure 6 shows a typical pressure history of the explosive gas element adjacent to the vehicle mass interface. The area under this curve multiplied by the vehicle area facing the explosive gases is the impulse delivered to the vehicle mass. The action time shown in this figure is less than 7 microseconds.

Figure 7 illustrates a typical history of the distribution of the detonation energy for the case of a free-expansion detonation. From this figure, it is seen that the largest fraction of energy is in the form of explosive gas kinetic energy expanding from the vehicle mass. It is noted that a substantial fraction of the detonation energy is residual to the vehicle mass as internal energy that must be dissipated within the vehicle structure.

#### EXPLOSIVE MASS STANDOFF

Shock-hydrodynamics calculations were completed to determine the effect of separating the explosive charge from the vehicle mass. The gas dynamic effect when the explosive gases are allowed to accelerate before impacting the vehicle mass should augment the impulse delivered.

Thus, the specific impulse performance and the velocity gained by the vehicle mass should be increased. Figure 8 displays the results of this parametric study for a free-expansion detonation. The data presented were taken at approximately 50 microseconds after initiation of the explosive charge. From Figure 8, it is seen that specific impulse performance is moderately affected by standoff distance,  $L^1$ , for a given explosive charge length,  $L$ . A particular  $L^1 / L$  ratio seems to exist for a given explosive mass to vehicle mass ratio which yields an optimum value of specific impulse. In Figure 8, these optimum values are connected with a dashed line. There is apparently a unique  $L^1 / L$  ratio for a given amount of explosive charge when compared to the vehicle mass at which momentum transfer to the vehicle mass is most efficient. The energy distributions for various  $L^1 / L$  ratios at a given mass ratio are not particularly discernible.

#### VELOCITY-BOOSTED CHARGES

Computer calculations were completed to determine the effect of "firing" an explosive charge at a vehicle mass which detonates enroute and, subsequently, expands from the vehicle mass. Explosive initiation locations of one explosive charge length and five explosive charge lengths from the vehicle mass were chosen. Figure 9 shows the effect on specific impulse of explosive charges given an initial velocity  $U_b$ . In Figure 9, mass ratio is the parameter. Initial explosive charge velocities greater than  $0.01 \text{ cm}/\mu\text{s}$  and  $0.03 \text{ cm}/\mu\text{s}$  for mass ratios of  $10^{-2}$  and  $10^{-1}$ , respectively, exceed the vehicle terminal velocity gained during the interaction with explosive gases expanding from rest.

The performance increase as a result of velocity-boosting explosive charges is appreciable. However, the vehicle mass absorbs a sizeable fraction of the kinetic energy associated with boosting the explosive charge. Unacceptable vehicle damage might result. Also, the practical utility of velocity-boosting an explosive charge must be considered.

## CONFINED DETONATIONS

The steady-state propulsion performance resulting from a detonation constrained from expansion by a recoil mass or an attenuator mass is given by solving Equations 1, 4 and 5 simultaneously, assuming the explosive gas density and velocity distribution. This is trivial in principle but algebraically tedious depending upon the complexity of the distributions chosen. For a constant gas density and a gas velocity distribution given by

$$u(x) = (U' + U) \frac{x}{L} - U \quad (17)$$

(implying a no-slip velocity condition at the interface between all solid masses and the gas),

$$U = \sqrt{2E_0} \sqrt{\frac{m/M}{1 + 1/3m/M + (M'/M + 1/3m/M) \left( \frac{M + m/2}{M' + m/2} \right)^2 - 1/3m/M \left( \frac{M + m/2}{M' + m/2} \right)}} \quad (18)$$

The specific impulse per explosive pulse follows from Equation 9. Equation 18 or Equation 9 inserted into Equation 9 may be plotted for various  $M'/M$ ,  $m/M$ , or other mass ratios using still other mass ratios as parameters (c. f., Figure 10).

Shock-hydrodynamics calculations were completed for many of the above such combinations. In addition, calculations were completed for cases where explosive charges were stacked between steel or aluminum materials of various thickness. These materials served as recoil mass and as attenuators to alter transmitted pressure waves. Up to seven explosive mass, recoil and attenuator mass, and vehicle mass stack combinations were used.

Figure 11 displays the effect on vehicle mass velocity of stacking Compound B explosive charges alternately between steel or aluminum

masses of various thickness. From Figure 11, it is seen that alternately stacking explosives between materials increases the vehicle mass velocity from the case of a single free-expansion detonation, for a given explosive mass. However, this performance gain is not comparable to the velocity gained simply by adding more explosive mass. That is, the effect on performance of constraining detonations by stacking inert masses between explosive charges is less than the performance effect associated with adding an equivalent amount of explosive mass. Still, by confining a detonation, a greater impulse is imparted to the vehicle mass, at a given mass ratio. The equivalent specific impulse (based upon the mass of explosive expended) is increased from the free-expansion detonation; however, the effective specific impulse (based upon the total mass expended) is decreased.

Figure 12 shows the history of the energy distribution for an explosive mass to vehicle mass ratio of approximately  $10^{-2}$  constrained from free expansion by a recoil mass of 0.1 of the vehicle mass. Comparing Figure 12 with Figure 7, it is seen that a greater fraction of the detonation energy is converted to vehicle mass kinetic energy, indicating that constraining the expansion of explosive gases improves energy conversion efficiency over the free-expansion detonation case. The confined explosive gases carry away little energy as kinetic energy and the recoil mass assumes this role and, additionally, absorbs energy. A significant fraction of the detonation energy is converted to vehicle mass internal energy which must be dissipated. Thus, increased energy conversion into vehicle mass kinetic energy is not accomplished without penalty. Figure 13 illustrates the magnitude of this penalty for  $m/M \cdot 10^{-2}$  as  $M'/M$  varies.

The effect on propulsion performance of confining a single explosive charge with a recoil mass is to increase the momentum exchange to the

vehicle over the free-expansion detonation case. However, again this performance gain is not comparable to the gain obtained by adding more explosive mass. Figure 14 illustrates the situation for  $m/M \sim 10^{-2}$  as  $M'/M$  varies, by comparison with the free-expansion detonation as  $m/M$  varies. Figure 14 displays computer results and steady-state results using Equations 11 and 18. Figure 10 shows the specific impulse performance for  $m/M \sim 10^{-2}$  as  $M'/M$  varies. The difference between equivalent and effective specific impulse is clear from this figure. Figure 10 might be compared with Figure 4.

Figure 15 shows the stagnation pressure history (or impulse) and the action times for  $m/M \sim 10^{-2}$  at various  $M'/M$  ratios. From this figure it is seen that the action time for a detonation propulsion system may be varied by confining the detonation. The use of delayed-detonation explosives might also serve this purpose. In addition, Figure 15 displays the impulse bounds of a detonation propulsion system: (1) a free-expansion detonation ( $M'/M = 0$ ), and (2) a completely confined detonation ( $M'/M = \infty$ ).

#### TOTALLY CONFINED DETONATIONS

The complete confinement of a detonation can be represented by allowing an explosive charge to be initiated between a rigid, motionless boundary and a vehicle mass. At the motionless boundary, by definition, the explosive gas velocity is zero for all time. The explosive gases must expand in the direction of motion of the center-of-mass of the vehicle. The use of this artifice allows the maximum momentum transfer to the vehicle mass and the greatest percentage conversion of detonation energy into vehicle kinetic energy, providing a theoretical upper limit on propulsion performance of a detonation propulsion system.

Figure 16 illustrates the distribution of detonation energy for a totally confined detonation where  $m/M \sim 10^{-2}$ . This figure can be compared with Figures 7 and 12. Figure 17 serves to contrast the explosive gas velocity distribution for the two cases: (1) the free-expansion detonation, where the

gases expand from the vehicle mass, and (2) the totally confined detonation, where the gases must expand in the direction of vehicle mass motion.

Returning to Figure 16, it is noted that a significant fraction of the detonation energy appears as vehicle mass internal energy. This increase in internal energy over the free-expansion detonation may be qualitatively examined by comparing the pressure histories associated with a totally confined detonation at a given  $m/M$  ratio with free-expansion detonations at various  $m/M$  ratios. Figure 18 serves this purpose. From Figure 18, it is seen that:

1. A totally confined detonation delivers an impulse greater than the impulse delivered from a free-expansion detonation using an order of magnitude more explosive for the free-expansion detonation.
2. The material pressures (or stresses) within the vehicle set up by a totally confined detonation are greater in magnitude and duration than the pressures resulting from a free-expansion detonation using an order of magnitude more explosive for the free-expansion detonation.

Clearly, the potential for vehicle damage and material spallation is great using completely confined explosives. For steel or aluminum, spallation should occur at a dynamic tensile strength of approximately 20 kilobars (Ref. 2).

Figures 19 and 20 compare the propulsion performance free-expansion detonations and totally confined detonations for various explosive mass to vehicle mass ratios. In Figure 19, both computer results and steady-state results are given. The steady-state results follow from Equations 11 and 18, where  $M^1/M \rightarrow \infty$  has been invoked. In Figure 20, the equivalent specific impulse has been used. Figure 20 contains computer results at, typically, 50 microseconds after initiation. For certain

applications, it is conceivable that the specific impulse performance from a detonation propulsion system may approach that of the totally confined detonation. For example, a vehicle employing explosive charges may be launched from an immobile platform, perhaps from the skin of a large space vehicle that has served its purpose.

## TEST RESULTS

Figure 20 also contains test data. Test data labeled No. 1 were taken from high-speed film and photoelectric timing wires. For these tests, a small square steel projectile was propelled by a thin explosive charge. The measurements were made milliseconds after detonation initiation. Data labeled No. 2 were taken from an X-ray camera (Ref. 1). Measurements were made over a few hundred microseconds interval approximately 3 centimeters downrange from the point where detonation initiation occurred. A sizeable detonator mass was used to initiate the explosive charge to propel a small steel bar and a recoil mass was used. Test data labeled No. 3 were taken from plates propelled by explosive slabs confined from behind by either a steel or a plywood wall. The care and precision with which all these tests were made and all data collected are unknown. In general, appreciable data scatter is notable in Figure 20.

## SECTION IV CONCLUSIONS AND RECOMMENDATIONS

The goal of this study, as previously stated, was to provide information to assess the potential of a detonation propulsion system. The findings herein provide information important to the determination of the limits of propulsion performance of a detonation propulsion system using plasticized charges. Consistent with one-dimensional, spallation-free analysis, the following was concluded.

1. A free-expansion detonation delivers a specific impulse comparable to that of a conventional chemical rocket. Specific impulse performance from a free-expansion detonation may be moderately increased by separating the explosive charge from the vehicle mass. Performance from a free-expansion detonation may be enhanced by giving the explosive charge an initial velocity. (However, this may be of marginal practical utility.)
2. Confining a detonation with a recoil mass, or stacking explosive charges between materials, increases propulsion performance from the free-expansion detonation, for a given explosive mass. This increase is not comparable to adding an equivalent mass of explosive. (Of course, for a given vehicle design, unacceptable vehicle damage may result when using more explosive charge.)
3. A totally confined detonation yields the maximum propulsion performance for a given explosive composition of fixed explosive mass. Vehicle damage and material spallation are likely when using a completely confined detonation.
4. Action times of the order of microseconds result when using explosive charges. The action time and also the impulse delivered from a detonation propulsion system for a given explosive may be varied by design.

Based upon the findings herein, further work is recommended. Careful experiments should be completed to determine the impulse delivered to

a mass from an explosive charge and, independently, the momentum exchange to the mass. The use of a simple ballistic pendulum technique is envisaged, although this method may not be simple in practice. An accelerometer may be mounted on the mass for corroborative measurement purposes and to verify action times. A variety of conditions should be experimentally studied. Additional experiments should be completed to determine material pressures (or stresses) set up within a mass struck by explosive gases. Again, a variety of conditions should be experimentally studied. Two-dimensional, shock-hydrodynamics calculations should be completed to guide these experiments, to attempt to correlate experimental findings, and to design a vehicle incorporating a detonation propulsion system. This vehicle should be tested to verify performance and to provide information for the firm design of a detonation propulsion system.

## REFERENCES

1. Aerojet General Corporation, "Explosive Propulsion," Unpublished Notes (February 1970).
2. Gross, M., Explosive Impulse Calculations, Report AFRPL-TR-71-2, November 1970.
3. Contract No. DAA-HO1-72-C-0530, United States Army to Aerojet General Corporation (1972).
4. Aziz, A.K., H. Hurwitz, and H. M. Sternberg, "Energy Transfer to a Rigid Piston under Detonation Loading," Physics of Fluids 4, pp 380-384 (March 1961).
5. Von Neumann, J., and R. D. Richtmyer, "A Method for the Numerical Calculation of Hydrodynamic Shocks," Journal of Applied Physics 21, pp 232-237 (March 1950).
6. Wilkins, M., et al., "A Computer Program for Calculating One-Dimensional Hydrodynamic Flow: KO Code," University of California Report 6919 (July 1962).
7. Van Splinter, P., Private Communication (AFRPL).

## AUTHORS' BIOGRAPHIES

ROBERT F. BESTGEN, CAPT, USAF  
Air Force Rocket Propulsion Laboratory

Ph.D degree, Astronautics, Air Force Institute of Technology

Capt Bestgen is a Laboratory Staff Scientist for the Technology Division, Special Projects Branch. He is currently engaged in evaluating advanced propulsion concepts and initiating advanced concept development programs.

JAMES R. NUNN, CAPT, USAF  
Air Force Rocket Propulsion Laboratory

M.S. degree, Engineering Physics, Air Force Institute of Technology

Capt Nunn is a Project Engineer in the Technology Division, Special Projects Branch. Currently, he is engaged in analyzing advanced propulsion concepts.

APPENDIX  
ILLUSTRATIONS

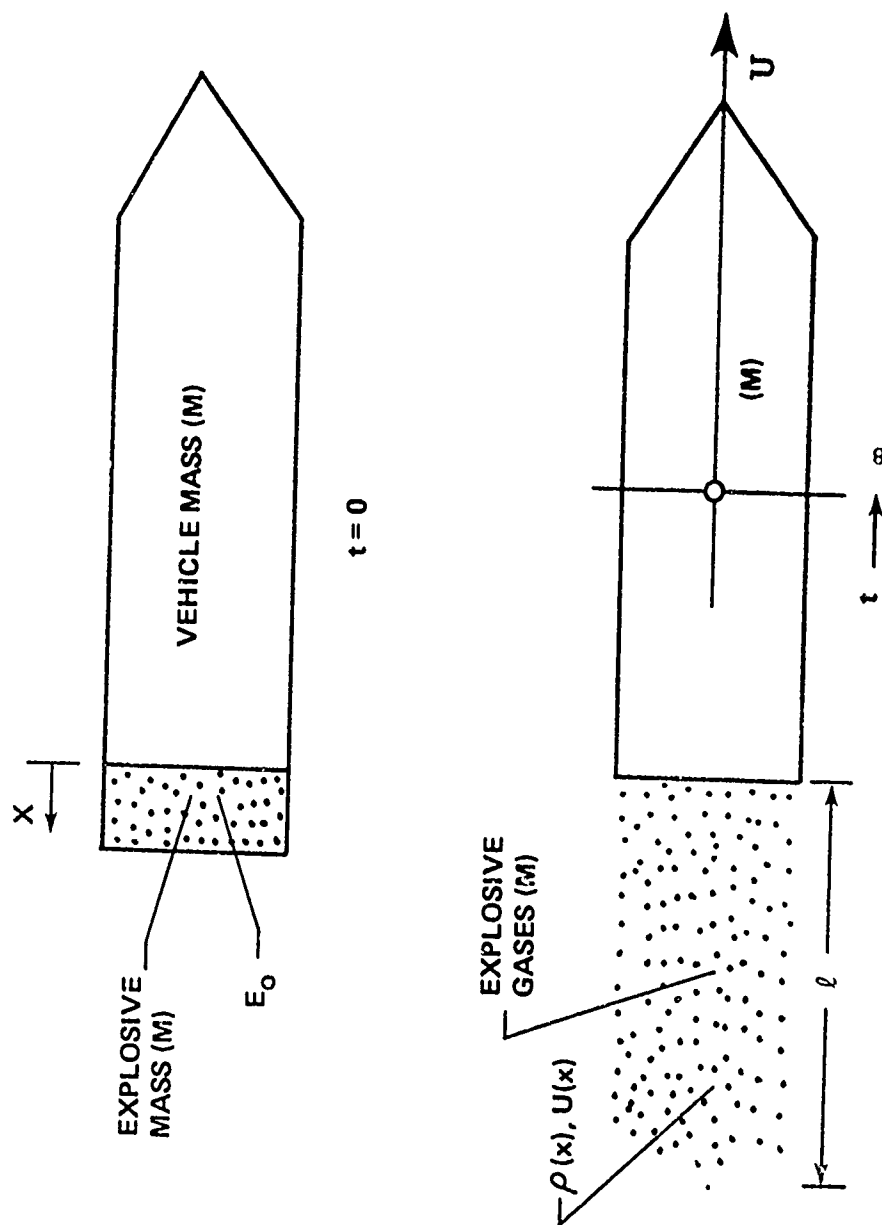


Figure 1. Detonation Propulsion System Schematic (Free-Expansion Detonation)

ICUASI-WUNCY 1 11 33 71

CYCLE	J	X(J,N)	U(J,N-1/2)	V(J+1/2,N)	P(J+1/2,N)	Q(J+1/2,N-1/2)	E(J+1/2,N)	MRARS-CC/CCO	AREAL(J,N)	DTSQ(1/2,1/2)	F(J+1/2,N)
184			CM/MICROSEC	CC/CCO	MEGABARS	MEGABARS				MICROSECS	
1	-4.89249E-01	-4.58000E-01	2.38784E 01	2.24626E-05	0.	3.03235E-03	1.812E-02	1.0000E-00	1.0000E-00	1.0000E-00	1.0000E-00
2	-3.69857E-01	-3.88952E-01	9.53326E 00	2.48273E-04	0.	1.33720E-03	6.546E-02	1.0000E-00	1.0000E-00	1.0000E-00	1.0000E-00
3	-3.22190E-01	-3.66255E-01	6.95023E 00	5.65041E-04	0.	2.21874E-03	2.097E-02	1.0000E-00	1.0000E-00	1.0000E-00	1.0000E-00
4	-2.87439E-01	-3.50756E-01	5.50373E 00	1.04711E-03	0.	3.25595E-03	8.965E-03	1.0000E-00	1.0000E-00	1.0000E-00	1.0000E-00
5	-2.59921E-01	-3.48436E-01	4.25060E 00	2.12819E-03	0.	5.11377E-03	3.435E-03	1.0000E-00	1.0000E-00	1.0000E-00	1.0000E-00
6	-2.36688E-01	-3.44065E-01	4.37417E 00	1.95903E-03	0.	4.84131E-03	3.836E-03	1.0000E-00	1.0000E-00	1.0000E-00	1.0000E-00
7	-2.16797E-01	-3.08493E-01	4.81029E 00	1.50696E-03	0.	4.09543E-03	5.442E-03	1.0000E-00	1.0000E-00	1.0000E-00	1.0000E-00
8	-1.92745E-01	-2.81340E-01	4.85397E 00	1.47351E-03	0.	4.04930E-03	5.616E-03	1.0000E-00	1.0000E-00	1.0000E-00	1.0000E-00
9	-1.68476E-01	-2.57633E-01	4.90695E 00	1.43332E-03	0.	3.97359E-03	5.835E-03	1.0000E-00	1.0000E-00	1.0000E-00	1.0000E-00
10	-1.43941E-01	-2.32580E-01	5.00040E 00	1.36420E-03	0.	3.85397E-03	6.249E-03	1.0000E-00	1.0000E-00	1.0000E-00	1.0000E-00
11	-1.18939E-01	-2.06676E-01	5.11537E 00	1.28523E-03	0.	3.71438E-03	6.785E-03	1.0000E-00	1.0000E-00	1.0000E-00	1.0000E-00
12	-9.36202E-02	-1.80092E-01	5.23948E 00	1.20685E-03	0.	3.57244E-03	7.431E-03	1.0000E-00	1.0000E-00	1.0000E-00	1.0000E-00
13	-6.71646E-02	-1.53022E-01	5.38827E 00	1.12067E-03	0.	3.41155E-03	8.191E-03	1.0000E-00	1.0000E-00	1.0000E-00	1.0000E-00
14	-4.2232E-02	-1.25338E-01	5.55679E 00	1.03289E-03	0.	3.24739E-03	9.172E-03	1.0000E-00	1.0000E-00	1.0000E-00	1.0000E-00
15	-1.2393E-02	-9.68627E-02	5.74279E 00	9.46092E-04	0.	3.06961E-03	1.035E-02	1.0000E-00	1.0000E-00	1.0000E-00	1.0000E-00
16	1.62747E-02	-6.74345E-02	5.95143E 00	8.60069E-04	0.	2.89189E-03	1.133E-02	1.0000E-00	1.0000E-00	1.0000E-00	1.0000E-00
17	4.60318E-02	-3.69371E-02	6.18426E 00	7.75856E-04	0.	2.71379E-03	1.359E-02	1.0000E-00	1.0000E-00	1.0000E-00	1.0000E-00
18	7.69531E-02	-5.27762E-03	6.45033E 00	6.92742E-04	0.	2.52440E-03	1.587E-02	1.0000E-00	1.0000E-00	1.0000E-00	1.0000E-00
19	1.09203E-01	2.77050E-02	6.74785E 00	6.13154E-04	0.	2.33756E-03	1.876E-02	1.0000E-00	1.0000E-00	1.0000E-00	1.0000E-00
20	1.42943E-01	9.23368E-02	7.07732E 00	5.38903E-04	0.	2.15479E-03	2.239E-02	1.0000E-00	1.0000E-00	1.0000E-00	1.0000E-00
21	1.78329E-01	9.86606E-02	7.45564E 00	4.67530E-04	0.	1.96956E-03	2.719E-02	1.0000E-00	1.0000E-00	1.0000E-00	1.0000E-00
22	2.15611E-01	1.36939E-01	7.91553E 00	3.97172E-04	0.	1.77617E-03	3.394E-02	1.0000E-00	1.0000E-00	1.0000E-00	1.0000E-00
23	2.53189E-01	1.77294E-01	8.49298E 00	3.27509E-04	0.	1.57148E-03	4.421E-02	1.0000E-00	1.0000E-00	1.0000E-00	1.0000E-00
24	2.97654E-01	2.23674E-01	9.18997E 00	2.63679E-04	0.	1.36904E-03	5.942E-02	1.0000E-00	1.0000E-00	1.0000E-00	1.0000E-00
25	3.43604E-01	2.67604E-01	1.00552E 01	2.05863E-04	0.	1.16947E-03	8.327E-02	1.0000E-00	1.0000E-00	1.0000E-00	1.0000E-00
26	3.93880E-01	3.19192E-01	1.111965E 01	1.53051E-04	0.	9.68154E-04	1.247E-01	1.0000E-00	1.0000E-00	1.0000E-00	1.0000E-00
27	4.49862E-01	3.76492E-01	1.28722E 01	1.04176E-04	0.	7.57617E-04	2.136E-01	1.0000E-00	1.0000E-00	1.0000E-00	1.0000E-00
28	5.14223E-01	4.42408E-01	1.54968E 01	6.25010E-05	0.	5.47211E-04	4.227E-01	1.0000E-00	1.0000E-00	1.0000E-00	1.0000E-00
29	5.91707E-01	5.21994E-01	2.08961E 01	2.84269E-05	0.	3.35902E-04	1.253E-01	1.0000E-00	1.0000E-00	1.0000E-00	1.0000E-00
30	6.96188E-01	6.30106E-01	4.07624E 01	7.94278E-02	6.62322E-02	3.03899E-01	5.256E-03	1.0000E-00	1.0000E-00	1.0000E-00	1.0000E-00
31	9.00000E-01	1.75923E-07	1.00000E 00	5.45941E-13	-0.	5.45941E-13	2.973E-02	1.0000E-00	1.0000E-00	1.0000E-00	1.0000E-00
32	1.00000E-00	-0.	1.00000E 00	0.	-0.	-0.	2.973E-02	1.0000E-00	1.0000E-00	1.0000E-00	1.0000E-00
33	1.00000E-00	-0.	1.00000E 00	0.	-0.	-0.	2.973E-02	1.0000E-00	1.0000E-00	1.0000E-00	1.0000E-00
61	3.90000E-00	0.	1.00000E 00	0.	0.	0.	2.973E-02	1.0000E-00	1.0000E-00	1.0000E-00	1.0000E-00

REGION MATERIAL K-ENERGY I-ENERGY MASS  
 1 6 0.10503E-01 C.18851E-02 0.25500E 00  
 2 15 0.60660E-14 -0. 0.23520E 02

V-CP= 0.58641E-08 CM/MICROSEC V-RMS= 0.22712E-07 CM/MICROSEC

Figure 2. Shock-Hydrodynamics Computer Printout

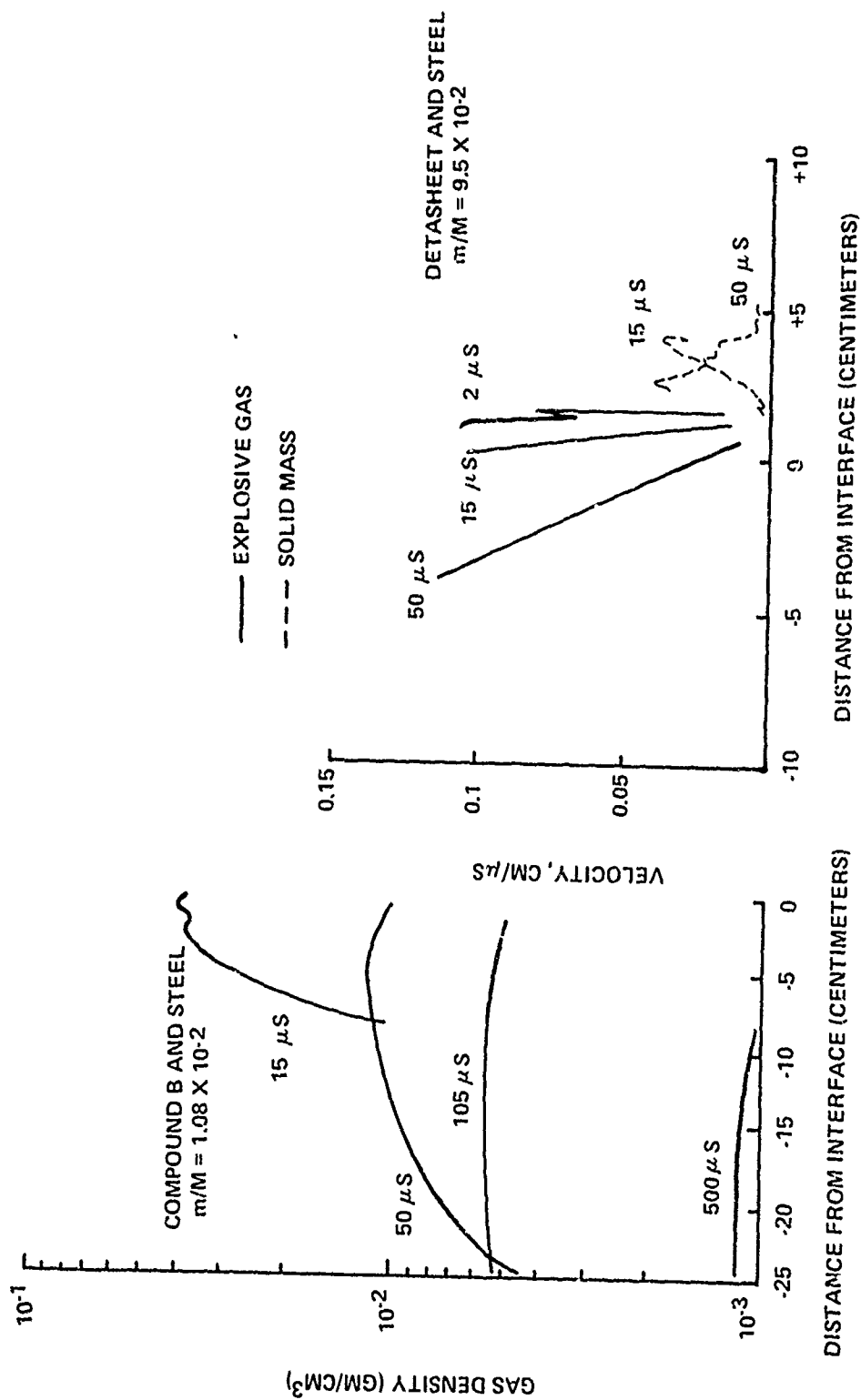


Figure 3. Free-Expansion Velocity and Density Distributions

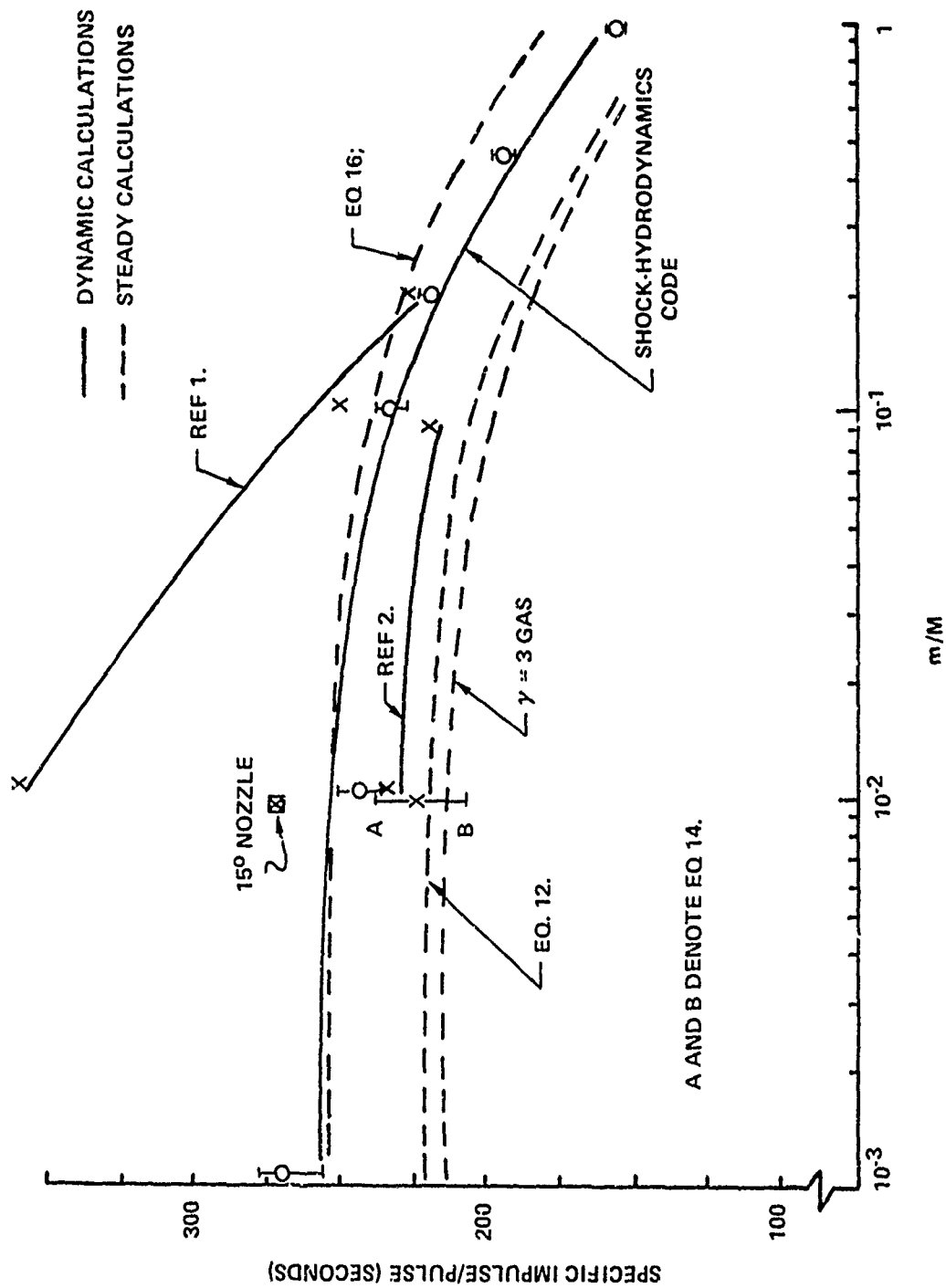


Figure 4. Free-Expansion Detonation Specific Impulse (Compound B and Steel)

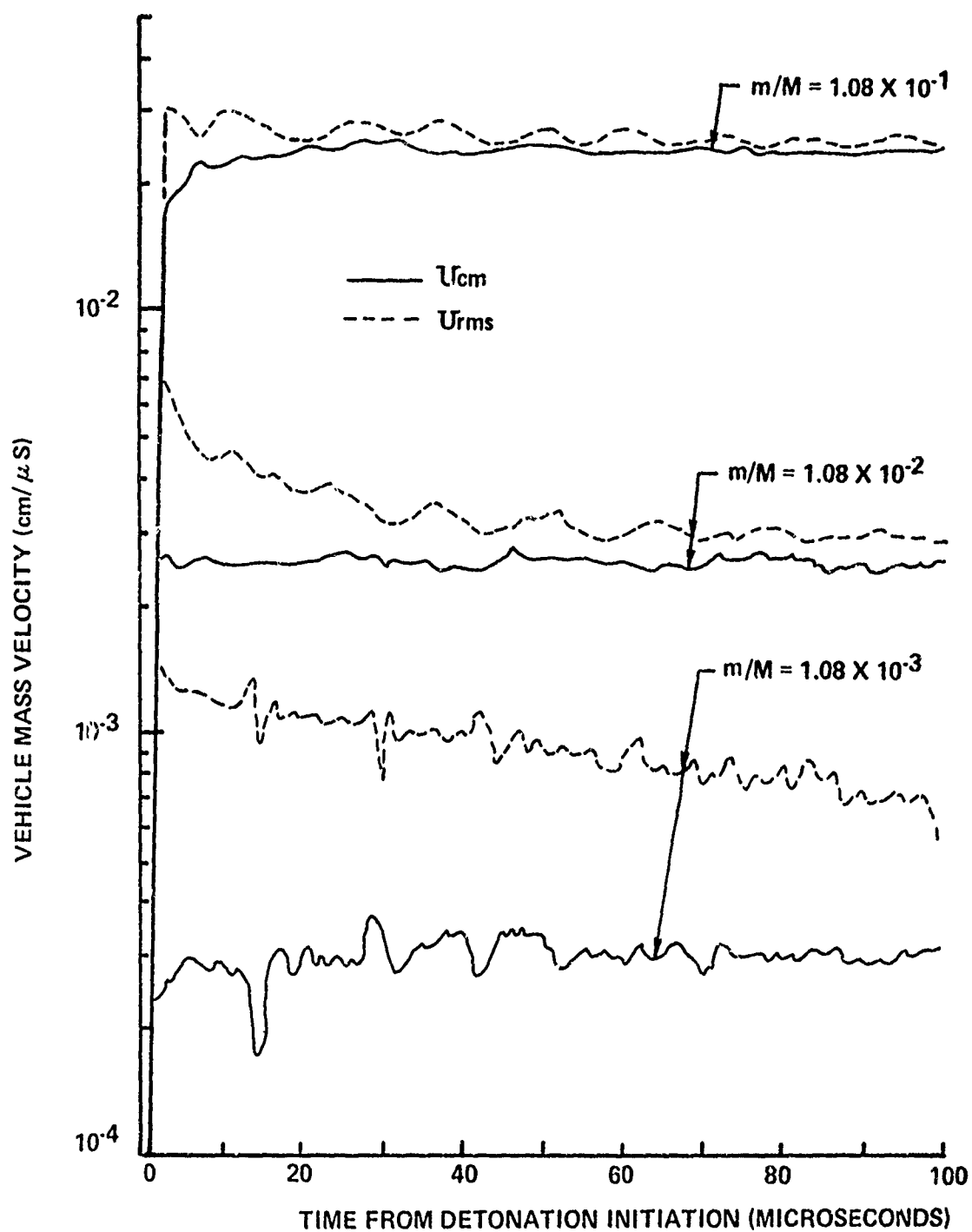


Figure 5. Vehicle Mass Velocity History  
(Compound B and Steel, Free-Expansion Detonation)

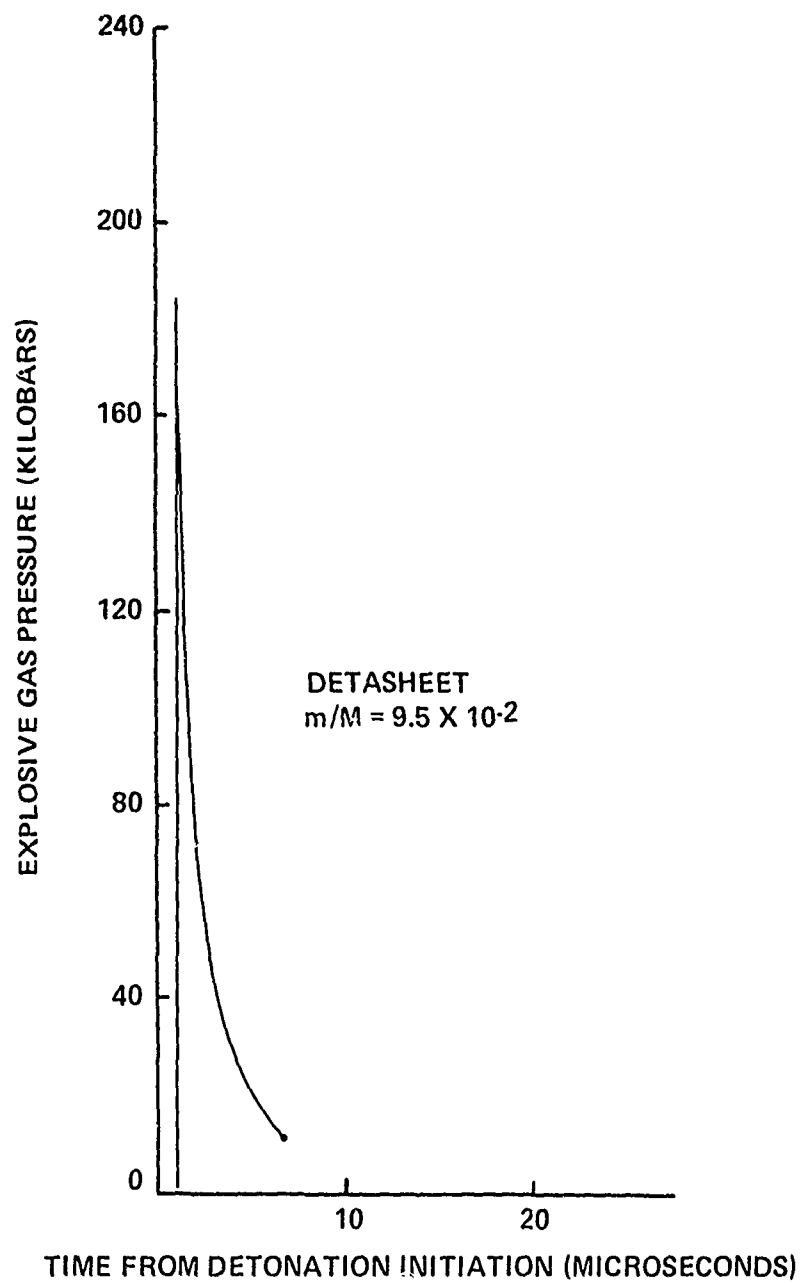


Figure 6. Pressure History (Free-Expansion Detonation)

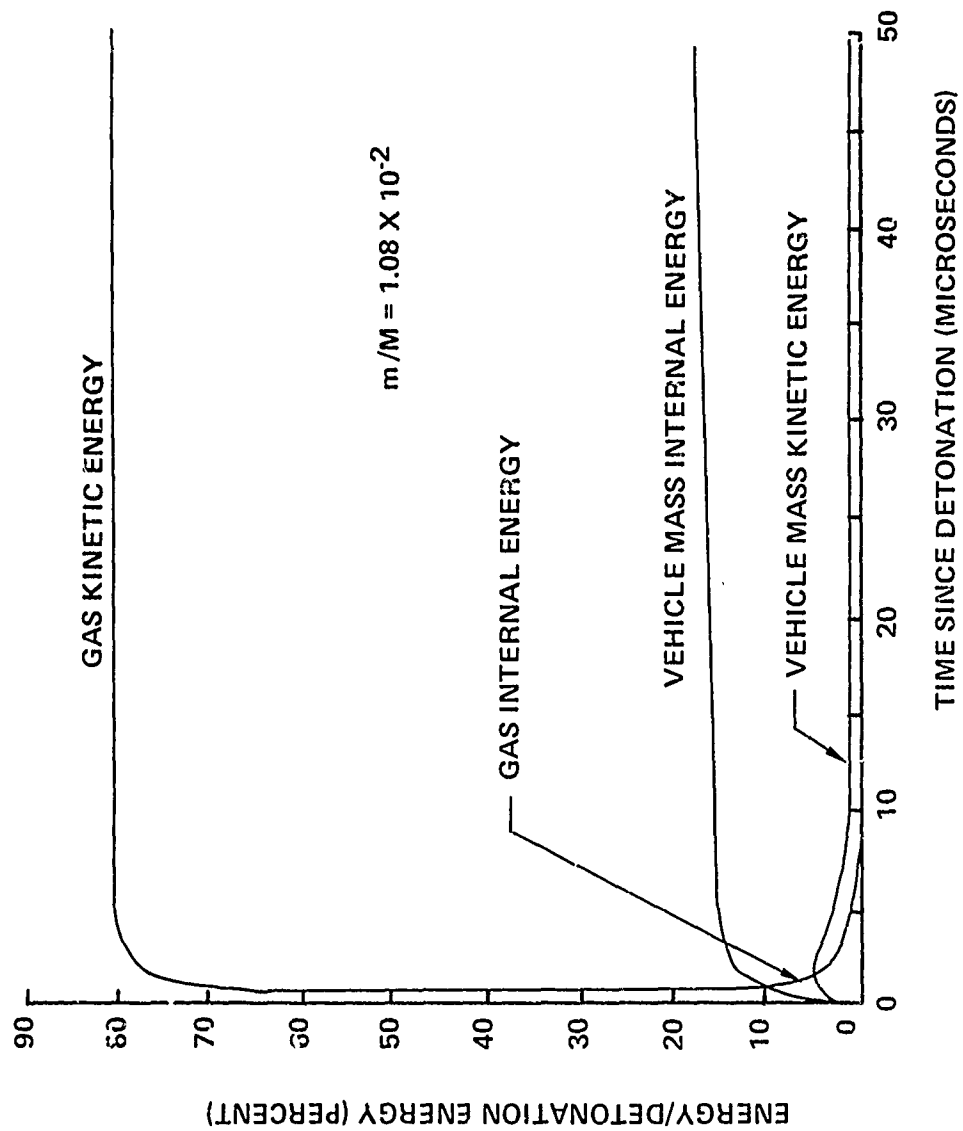


Figure 7. Energy History (Compound B and Steel, Free-Expansion Detonation)

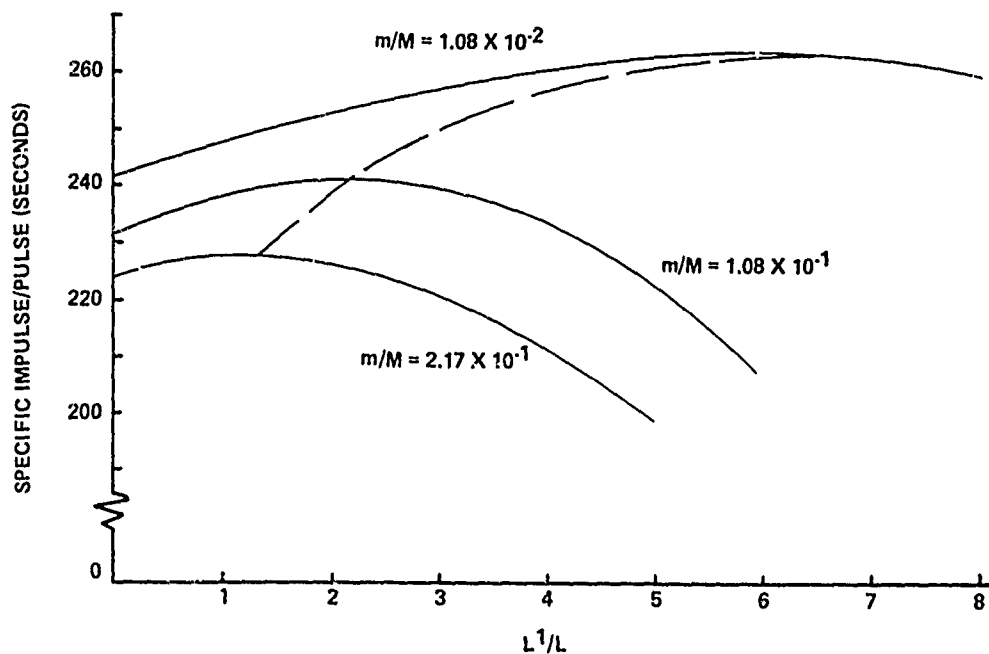


Figure 8. Explosive Mass Standoff Performance (Compound B and Steel)

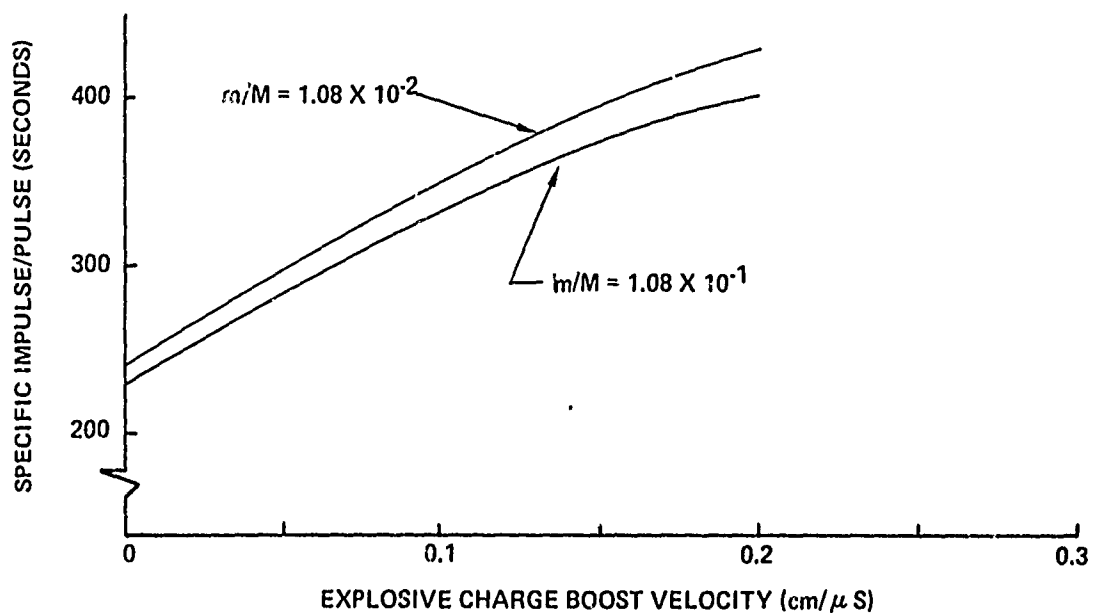


Figure 9. Velocity-Boosted Performance (Compound B and Steel)

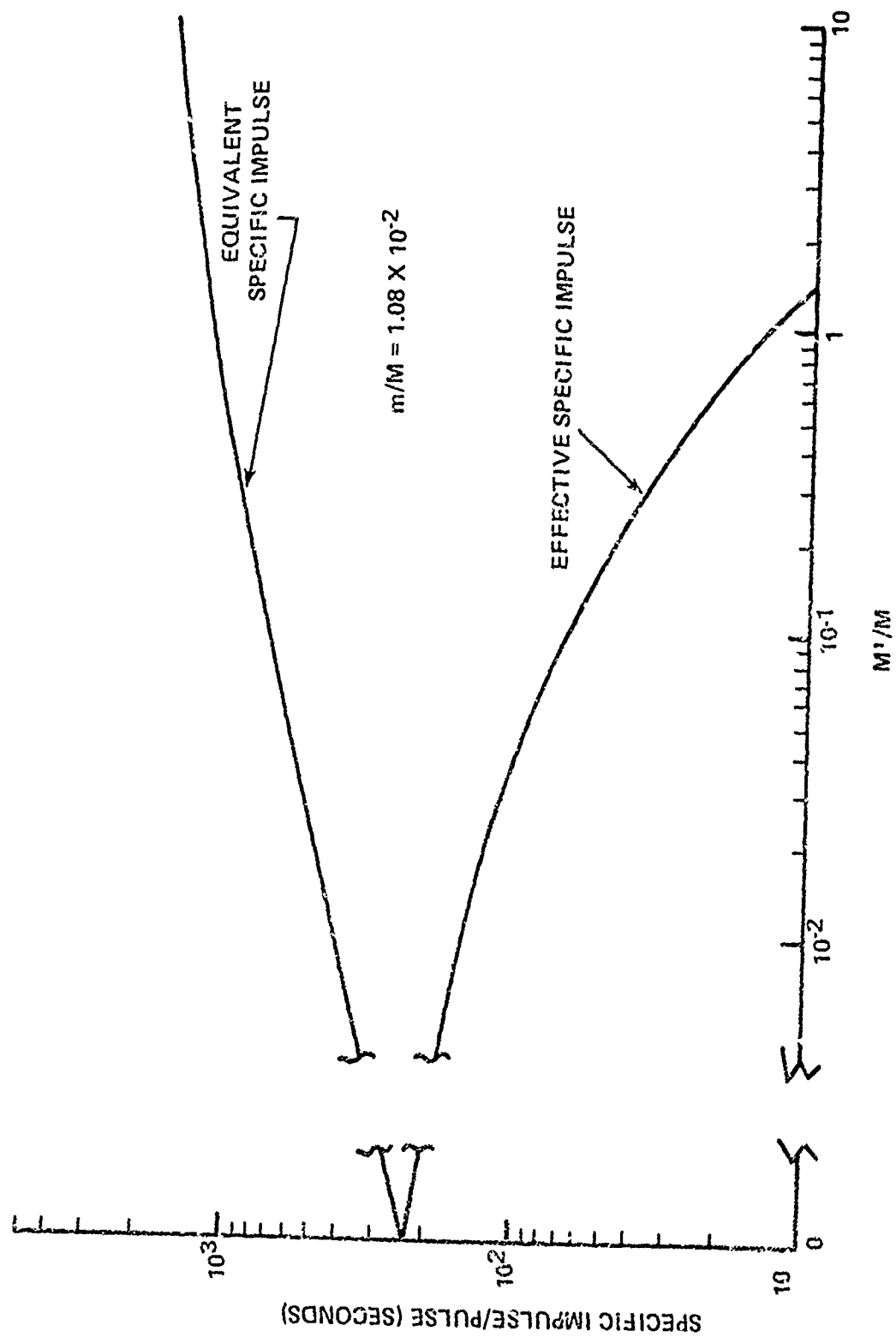


Figure 10. Confined Detonation Specific Impulse Performance (Compound B and Steel)

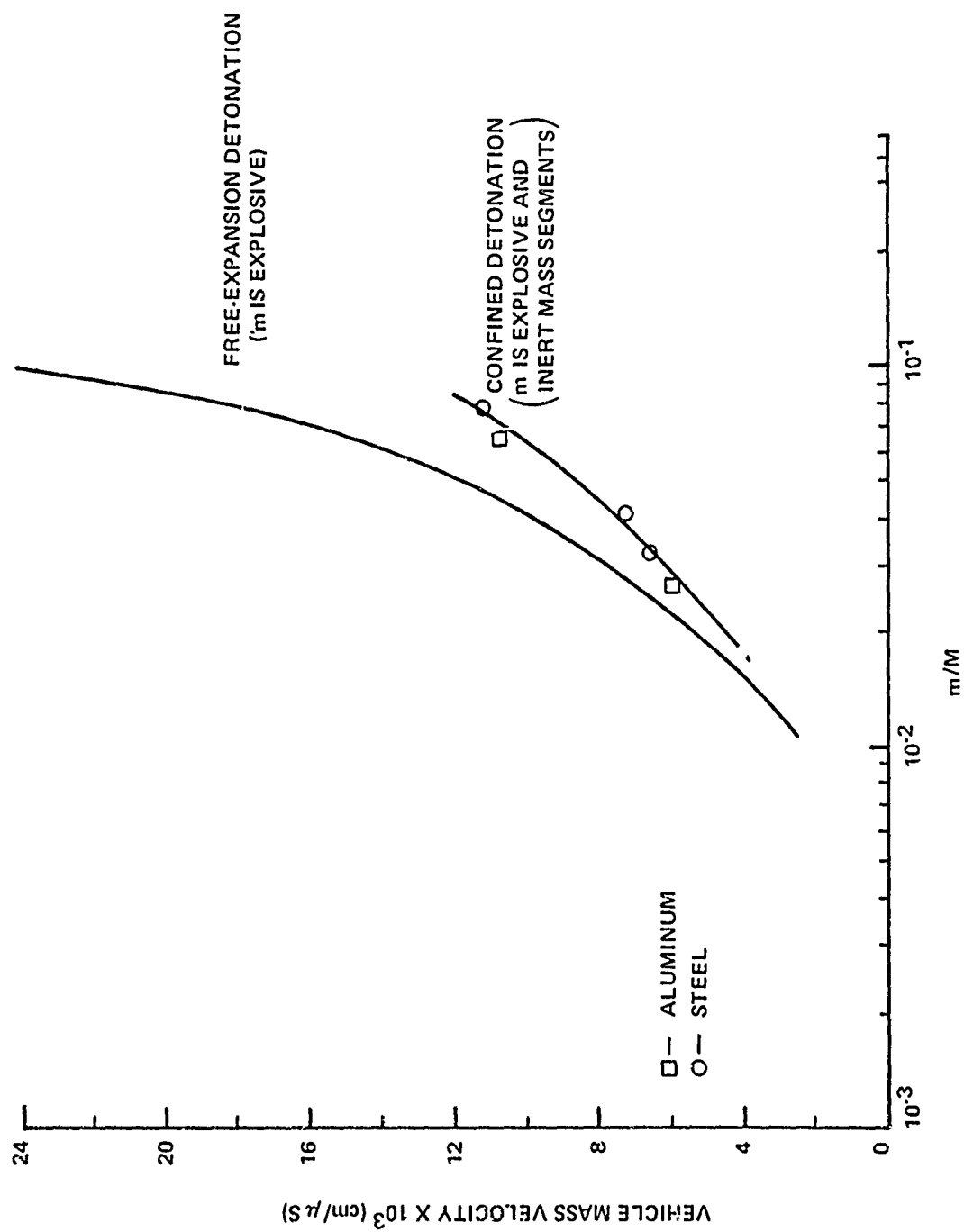


Figure 11. Stacked Explosives Performance Comparison (Compound B)

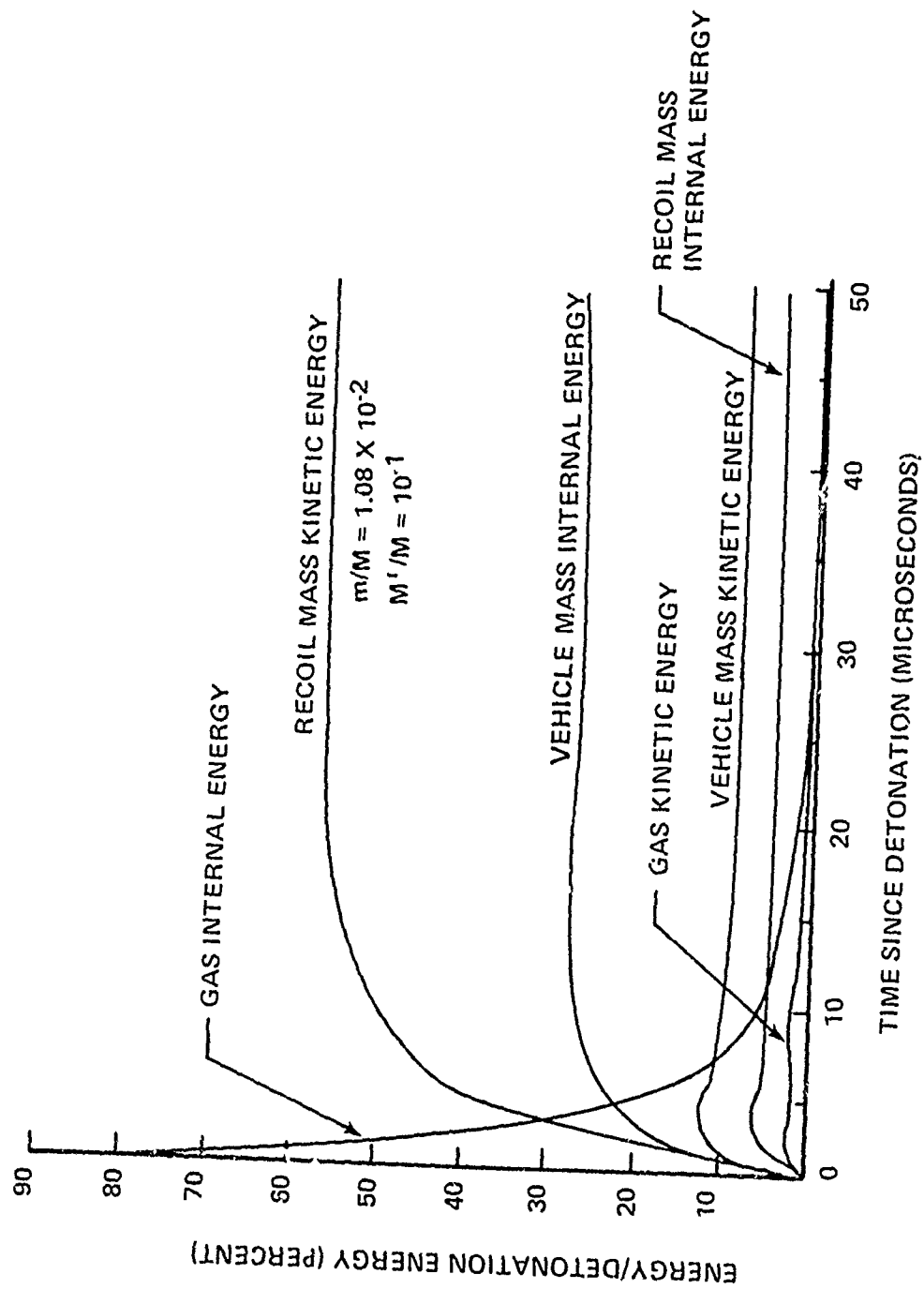


Figure 12. Energy History (Compound B and Steel, Confined Detonation)

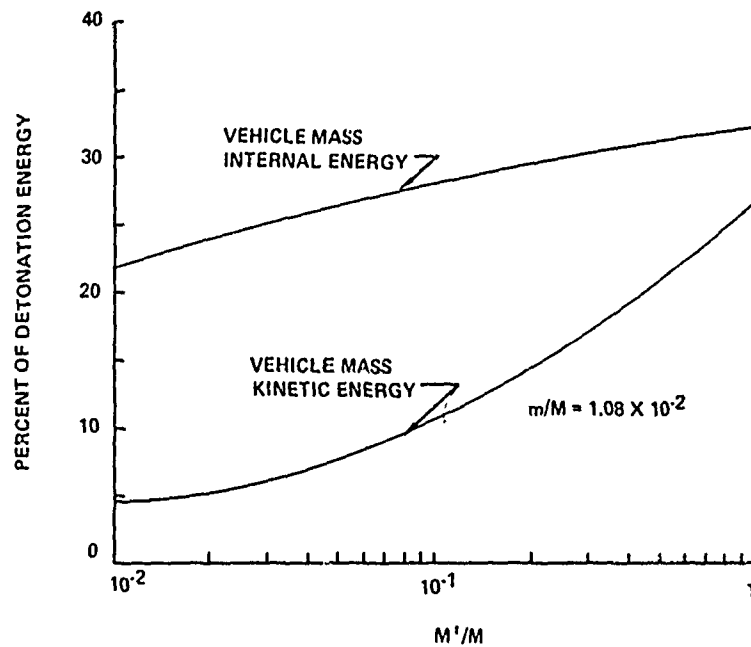


Figure 13. Effect of Recoil Mass on Vehicle Mass Energy (Compound B and Steel, Confined Detonation)

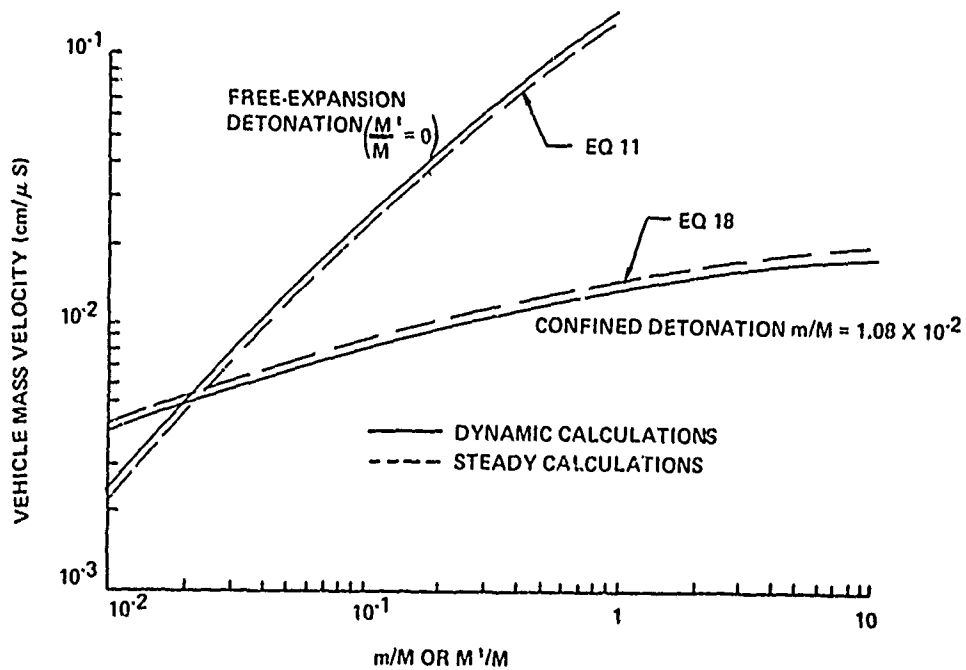


Figure 14. Effect of Recoil Mass on Vehicle Mass Velocity (Compound B and Steel)

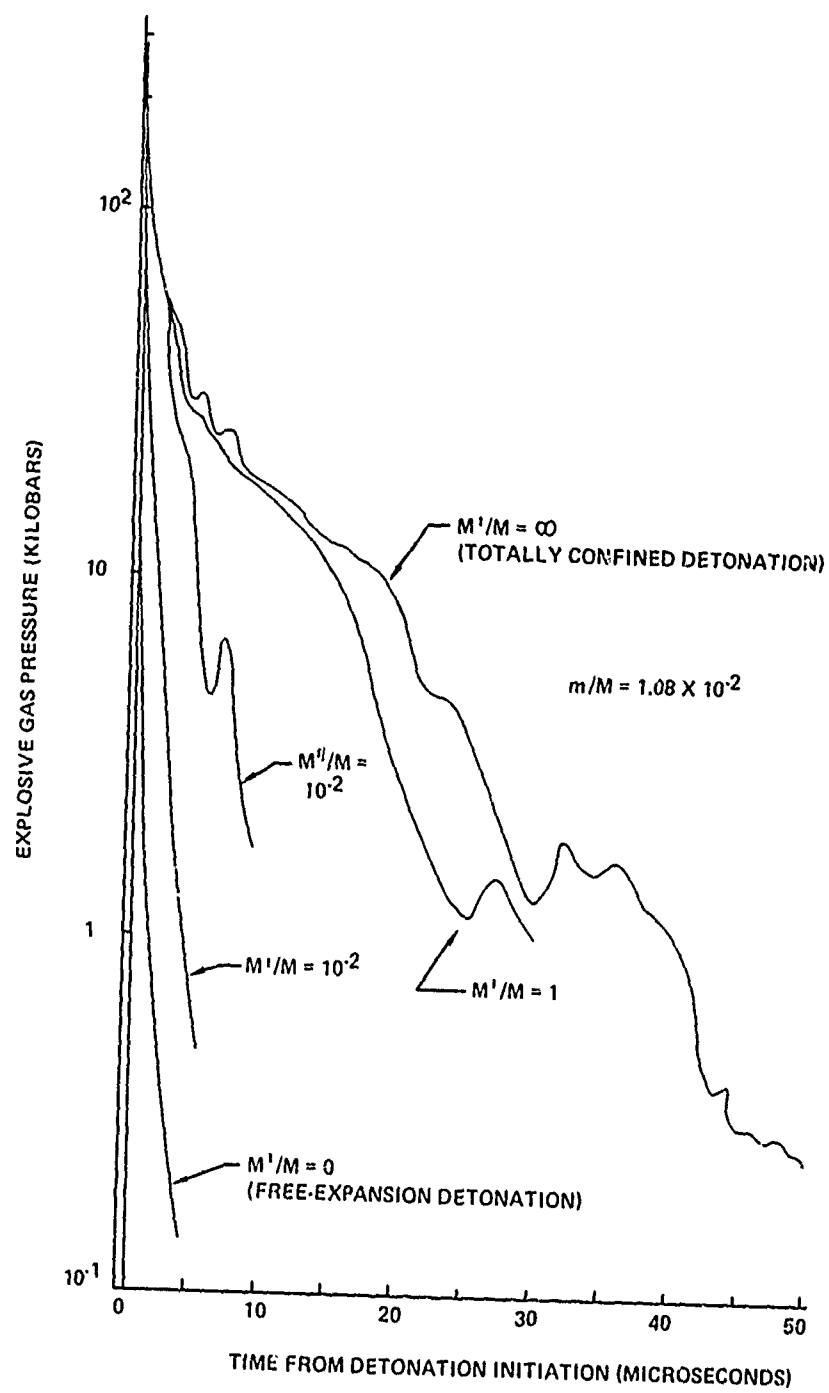


Figure 15. Pressure History Comparisons  
(Compound B and Steel)

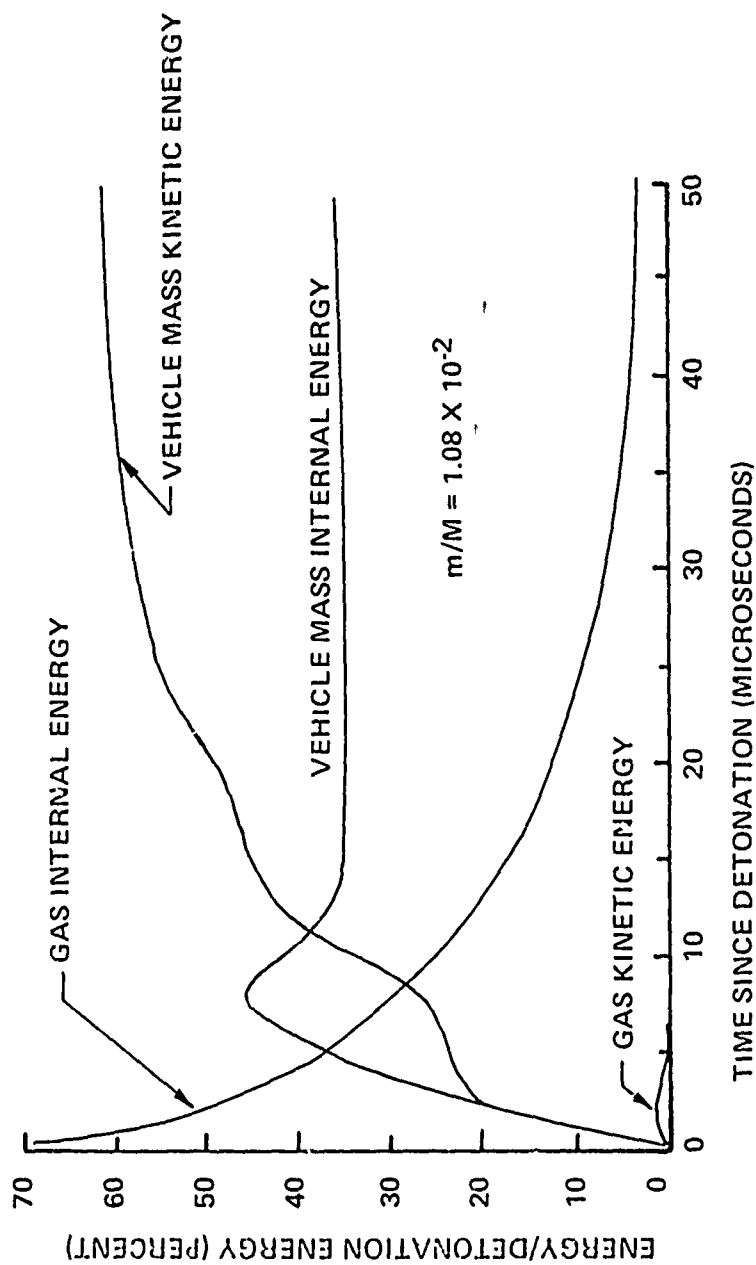


Figure 16. Energy History (Compound B and Steel, Totally Confined Detonation)

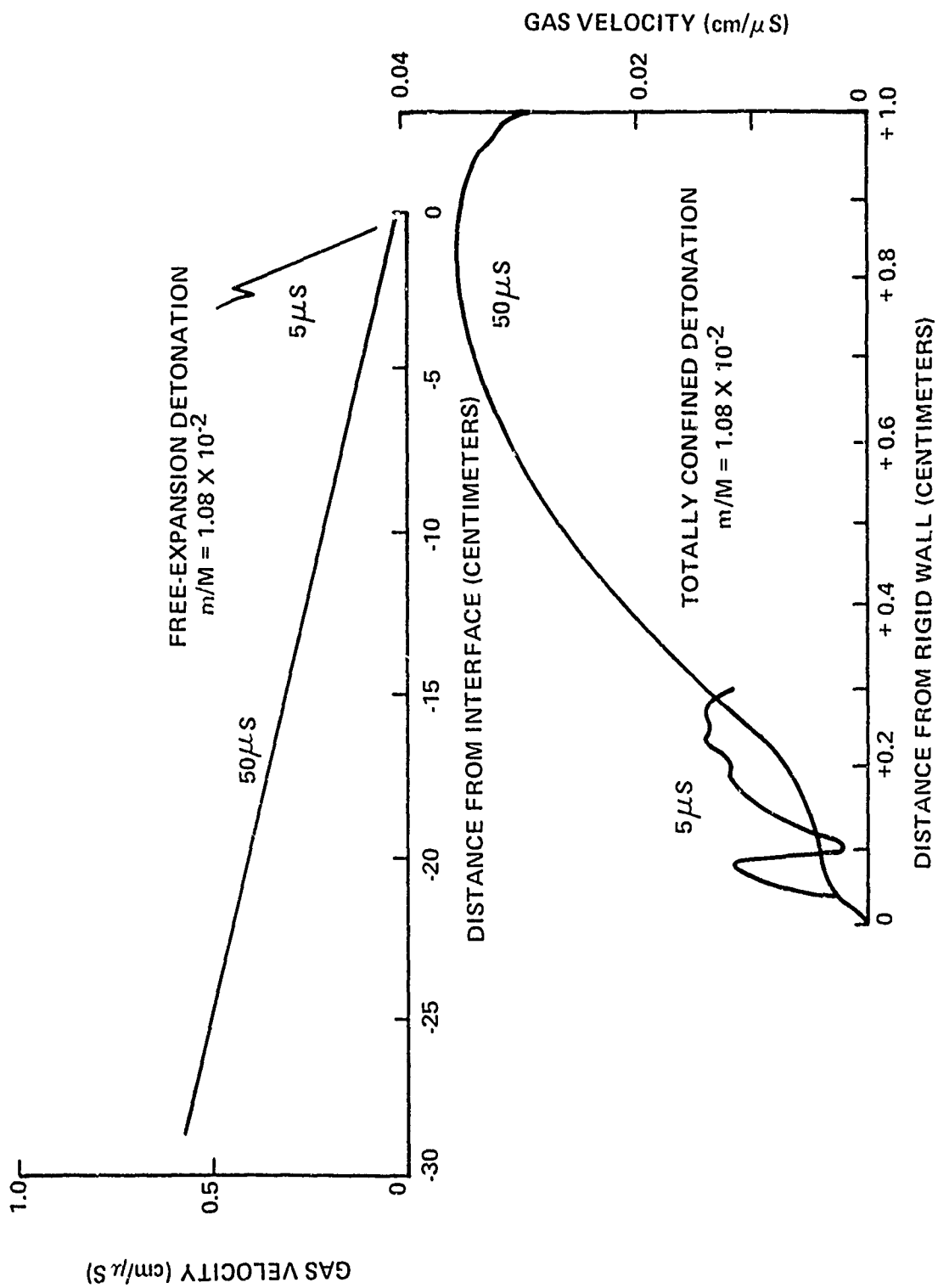


Figure 17. Velocity Distribution Comparison (Compound B and Steel)

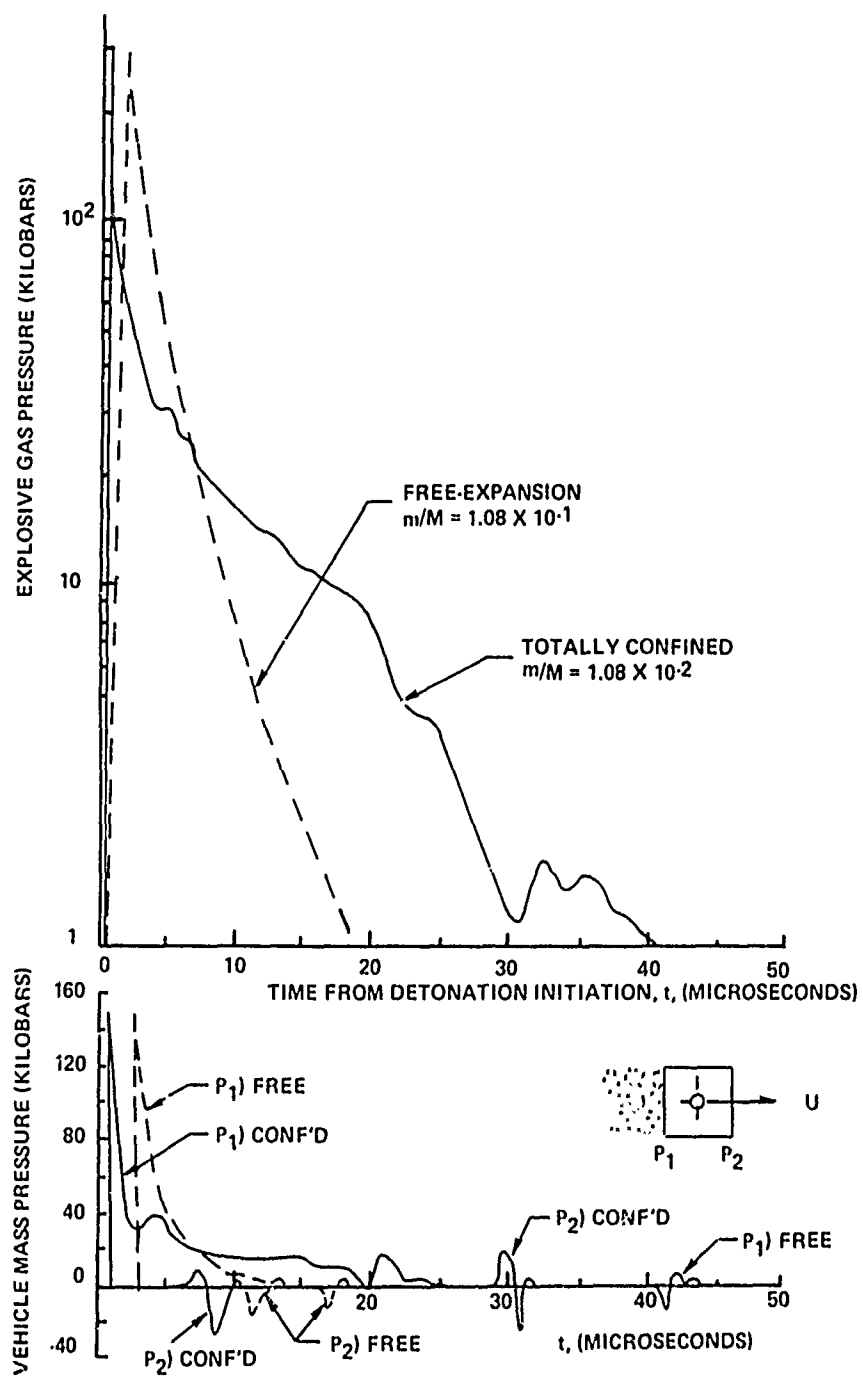


Figure 18. Pressure History Comparison (Compound B and Steel)

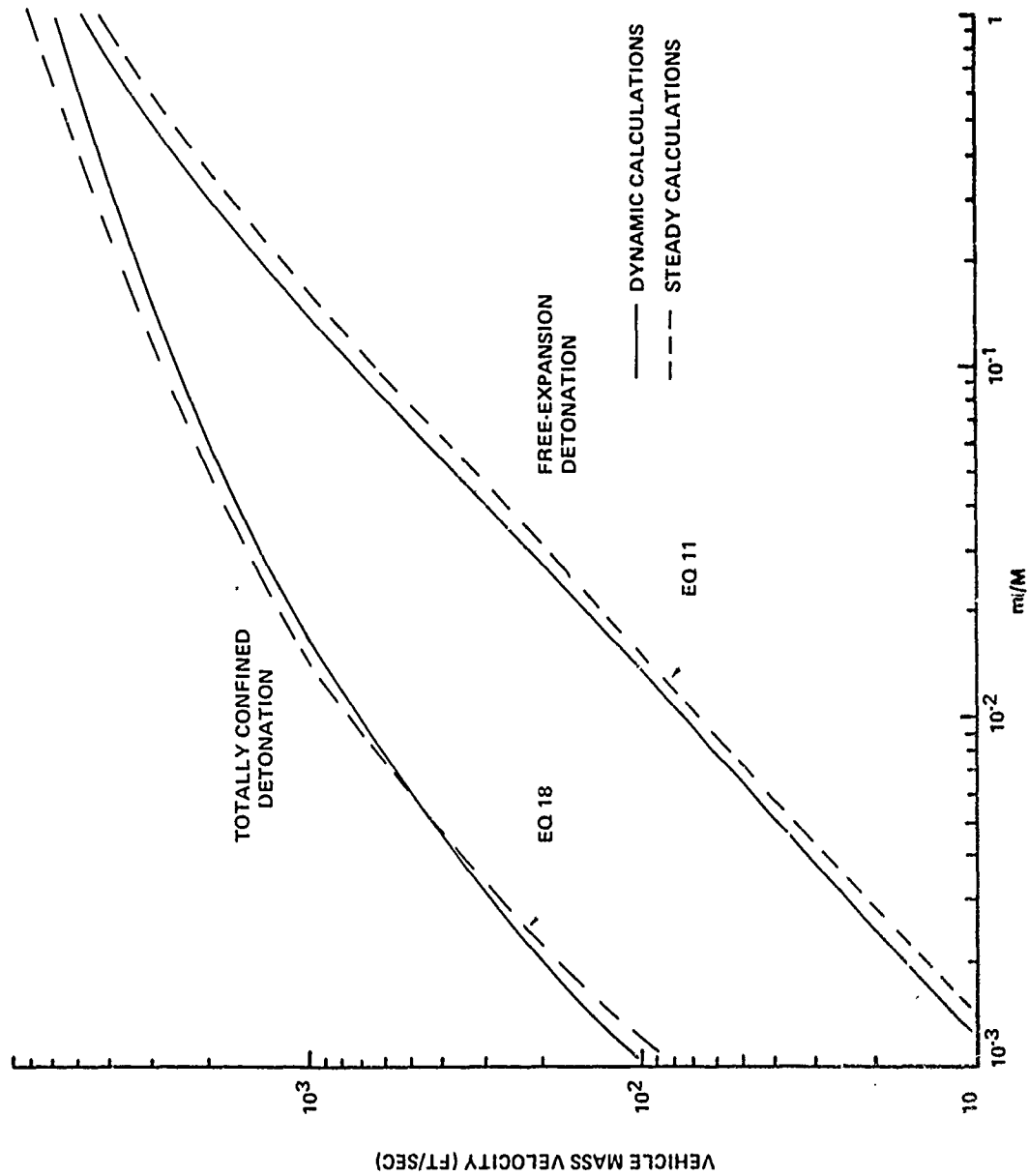


Figure 19. Vehicle Mass Velocity Comparison (Compound B and Steel)

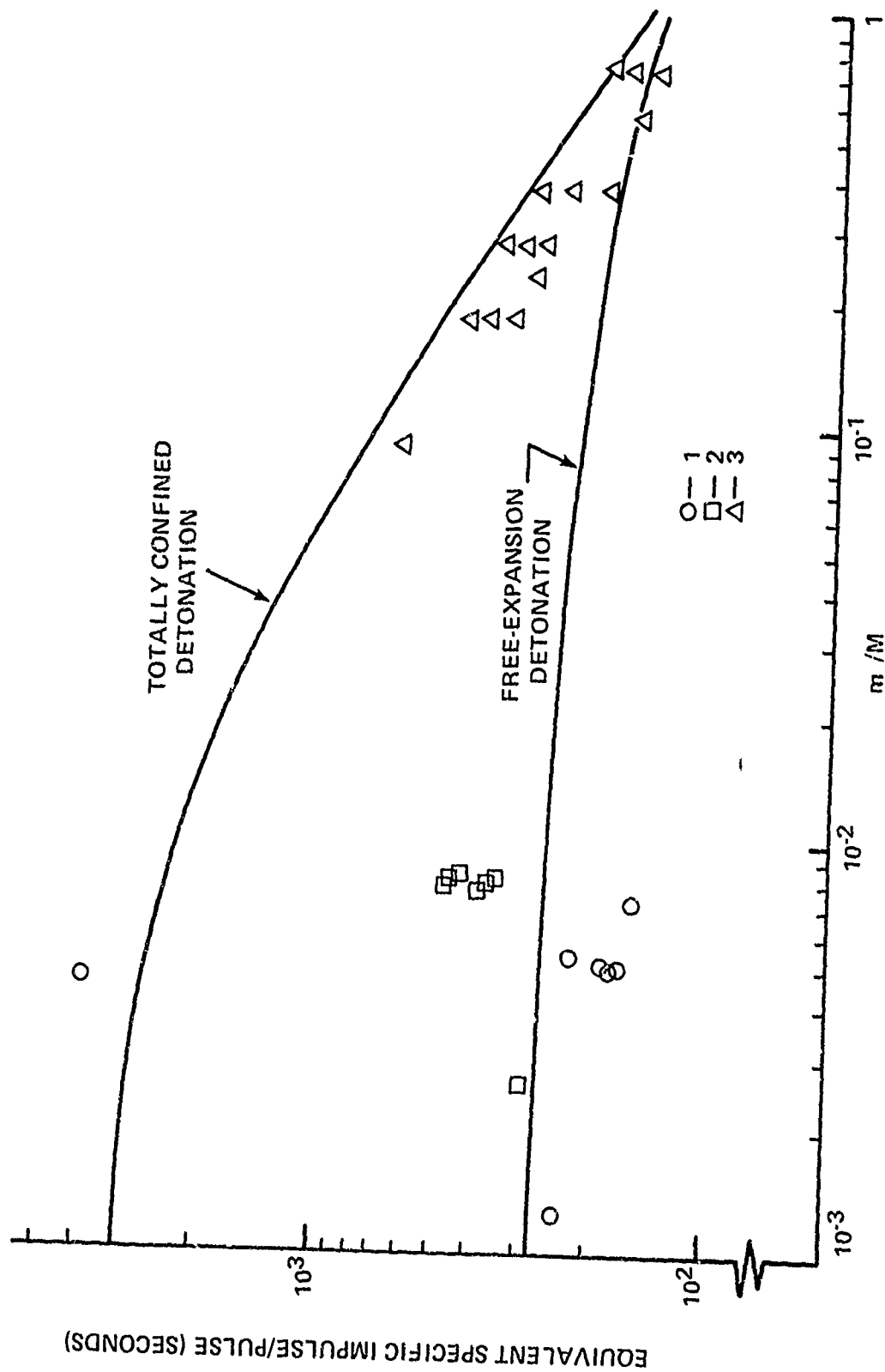


Figure 20. Specific Impulse Comparison (Compound B and Steel)

UNCLASSIFIED

Security Classification

DOCUMENT CONTROL DATA - R & D		
(Security classification of title, body of abstract and indexing annotation must be entered when the overall report is classified)		
1. ORIGINATING ACTIVITY (Corporate author) Air Force Rocket Propulsion Laboratory, Edwards, California		2a. REPORT SECURITY CLASSIFICATION Unclassified
		2b. GROUP
3. REPORT TITLE  A Study of the Propulsion Performance from Plasticized Explosives		
4. DESCRIPTIVE NOTES (Type of report and inclusive dates) Technical Report (October 1971 - May 1972)		
5. AUTHOR(S) (First name, middle initial, last name) Capt R. R. Bestgen Capt J. R. Nunn		
6. REPORT DATE August 1972	7a. TOTAL NO. OF PAGES 44 & vi	7b. NO. OF REFS 7
8a. CONTRACT OR GRANT NO.	9a. ORIGINATOR'S REPORT NUMBER(S)  AFRPL-TR-72-56	
b. PROJECT NO.		
c.	9b. OTHER REPORT NO(S) (Any other numbers that may be assigned this report)	
d.		
10. DISTRIBUTION STATEMENT This document has been approved for public release and sale; its distribution is unlimited.		
11. SUPPLEMENTARY NOTES	12. SPONSORING MILITARY ACTIVITY Air Force Rocket Propulsion Laboratory Air Force Systems Command, USAF Edwards, California 93523	
13. ABSTRACT  INSERT A - See attachment.		

DD FORM 1 NOV 65 1473

43

UNCLASSIFIED

Security Classification

UNCLASSIFIED

Security Classification

14. KEY WORDS	LINK A		LINK B		LINK C	
	ROLE	WT	ROLE	WT	ROLE	WT
Explosives Explosive-Propulsion Shock-Hydrodynamics Detonation-Propulsion Plasticized Explosives						

UNCLASSIFIED

Security Classification

## INSERT A

A theoretical study was made to determine the performance of a detonation propulsion system using plasticized explosives. Steady-state and shock-hydrodynamic calculations were completed for : (1) free-expansion detonations, where the explosive gases are free to expand from the vehicle mass after impacting the vehicle, (2) confined detonations, where recoil mass or attenuator mass is used to constrain the expansion, and (3) totally confined detonations, where the momentum transfer to the vehicle mass and the conversion of detonation energy into vehicle kinetic energy are maximized. The effects upon propulsion performance of separating explosive charges from the vehicle mass, giving the explosive charge an initial velocity, and stacking explosive charges between solid materials, were also studied. Results show that a free-expansion detonation delivers a specific impulse comparable to that of a conventional chemical rocket using solid propellant. Separating the explosive charge from the vehicle can result in a moderate increase in the performance of a detonation propulsion system. Giving the explosive an initial velocity also increases performance, although this may be of marginal practical utility. Partially confining a detonation with material increases the momentum transfer to the vehicle and the vehicle's kinetic energy, but the confinement is not comparable to adding an equivalent amount of explosive mass. Stacking explosives between materials leads to a similar result. A totally confined detonation delivers the maximum performance from a detonation propulsion system, but vehicle damage is likely when using a totally confined detonation. The results indicate that the detonation propulsion concept is feasible for special purpose applications where the specific impulse required is about 250 to 300 seconds.